Assessing effects of germline exposure to environmental toxicants by high-throughput screening in *C. elegans*

Nara Shin[1], Luciann Cuenca[1], Rajendiran Karthikraj[2], Kurunthachalam Kannan[2,3], Monica P. Colaiácovo[1]*

1 Department of Genetics, Harvard Medical School, Boston, MA, United States of America, **2** Wadsworth Center, New York State Department of Health, Empire State Plaza, Albany, New York, United States of America, **3** Department of Environmental Health Sciences, School of Public Health, University at Albany, State University of New York, Albany, New York, United States of America

* mcolaiacovo@genetics.med.harvard.edu

Abstract

Chemicals that are highly prevalent in our environment, such as phthalates and pesticides, have been linked to problems associated with reproductive health. However, rapid assessment of their impact on reproductive health and understanding how they cause such deleterious effects, remain challenging due to their fast-growing numbers and the limitations of various current toxicity assessment model systems. Here, we performed a high-throughput screen in *C. elegans* to identify chemicals inducing aneuploidy as a result of impaired germline function. We screened 46 chemicals that are widely present in our environment, but for which effects in the germline remain poorly understood. These included pesticides, phthalates, and chemicals used in hydraulic fracturing and crude oil processing. Of the 46 chemicals tested, 41% exhibited levels of aneuploidy higher than those detected for bisphenol A (BPA), an endocrine disruptor shown to affect meiosis, at concentrations correlating well with mammalian reproductive endpoints. We further examined three candidates eliciting aneuploidy: dibutyl phthalate (DBP), a likely endocrine disruptor and frequently used plasticizer, and the pesticides 2-(thiocyanomethylthio) benzothiazole (TCMTB) and permethrin. Exposure to these chemicals resulted in increased embryonic lethality, elevated DNA double-strand break (DSB) formation, activation of p53/CEP-1-dependent germ cell apoptosis, chromosomal abnormalities in oocytes at diakinesis, impaired chromosome segregation during early embryogenesis, and germline-specific alterations in gene expression. This study indicates that this high-throughput screening system is highly reliable for the identification of environmental chemicals inducing aneuploidy, and provides new insights into the impact of exposure to three widely used chemicals on meiosis and germline function.

Author summary

The ever-increasing number of new chemicals introduced into our environment poses a significant problem for risk assessment. In addition, assessing the direct impact of

toxicants on human meiosis remains challenging. We successfully utilized a high-throughput platform in the nematode *C. elegans*, a genetically tractable model organism which shares a high degree of gene conservation with humans, to identify chemicals that affect the germline leading to aneuploidy. We assessed chemicals that are highly prevalent in the environment in worms carrying a fluorescent reporter construct allowing for the identification of X chromosome nondisjunction combined with a mutation increasing cuticle permeability for analysis of low doses of exposure. Follow up analysis of three chemicals: DBP, permethrin and TCMTB, further validated the use of this strategy. Exposure to these chemicals resulted in elevated levels of DNA double-strand breaks, activation of a DNA damage checkpoint, chromosome morphology defects in late meiotic prophase I as well as impaired early embryogenesis and germline-specific changes in gene expression. Our results support the use of this high-throughput screening system to identify environmental chemicals inducing aneuploidy, and provide new insights into the effects of exposure to DBP, permethrin, and TCMTB on meiosis and germline function.

Introduction

Man-made environmental chemicals such as phthalates, bisphenols, and pesticides, continue to increase in numbers, and some of them have been linked to reproductive problems [1–5]. However, rapidly identifying chemicals that impact reproductive health and understanding how they interfere with meiosis remains challenging. This is partly due to the fact that meiosis is not easily recapitulated in a tissue culture setting and that female mammalian meiosis can span from several months in mice to decades in humans. Failure to achieve accurate chromosome segregation during meiosis causes aneuploidy and can lead to infertility, stillbirths, miscarriages and birth defects [6,7]. Thus, high-throughput screens to assess the impact of environmental chemicals on reproductive health have been in high demand. *C. elegans* is a genetically and molecularly tractable model organism that provides many advantages for the study of meiosis and its use in high-throughput screens, including sharing a high degree of conservation of its genes and biochemical pathways with humans, carrying a well defined and characterized germline, a rapid life cycle (it develops from an egg into an adult in approximately 3 days at 20°C) and low maintenance costs [8–14].

Using chemotherapeutic agents and environmental compounds from the ToxCast Phase I library with comprehensive mammalian *in vivo* end point data (ToxRef database), we previously demonstrated that a *Pxol-1::gfp* transcriptional reporter strain in *C. elegans* can be used to identify chemicals inducing embryonic aneuploidy. Moreover, we showed that this approach is highly predictive of mammalian reproductive toxicity (balanced accuracy rate of 70%; this value corresponds to the average of sensitivity (correct identification of true positives) and specificity (correct identification of true negatives)) [15]. Here, for the first time, we successfully combined the use of this strain with sorting of live worms based on fluorescence intensity with a large object flow cytometry system, the COPAS Biosort (Union Biometrica), in a high-throughput screen. We screened a library of 46 chemicals consisting of pesticides, phthalates, and chemicals used in hydraulic fracturing and crude oil processing, selected based on their widespread presence in the environment and yet not well understood effects on the germline. Nineteen of these chemicals led to a GFP signal fold ratio over vehicle alone that was higher than the levels detected for bisphenol A (BPA) exposure, a widely used plasticizer and endocrine disruptor previously shown to affect meiosis in worms and mammals [1,16–20]. Three of these chemicals, dibutyl phthalate (DBP), permethrin and 2-(thiocyanomethylthio) benzothiazole (TCMTB), all high production volume chemicals, were evaluated further to

validate the screening platform and gain insight into how they interfere with events in the germline.

DBP is a phthalate ester widely used as either a solvent or plasticizer. Therefore, it is found in a variety of items such as personal care products, plastic food wraps, the enteric-coatings of solid oral drug products, adhesives, and printing inks. DBP is highly prevalent in the environment and its estimated daily intake for the general population is 7–10 μg/kg/day [21–23]. Higher levels have been detected in human urine, follicular fluid, and serum in different occupationally exposed groups [21,24]. *In vitro* and animal studies have shown that DBP disrupts the reproductive system resulting in inhibition of ovarian antral follicle growth and viability, altered gene expression in ovaries, testicular malformation and dysfunction, inhibition of spermatogenesis, and altered androgen signaling in males [25–28]. In humans, a significant inverse relationship has been observed between levels of DBP metabolites (i.e. mBP) in prenatal urine and male anogenital distance [29]. Permethrin, a synthetic pyrethroid insecticide, is commonly used for crop protection and the treatment of head lice and scabies, since it is considered to have low toxicity compared to other insecticides [30]. Permethrin enters the body through skin, inhalation, and oral uptake. This chemical has been detected in adults and children [31–34] and its major metabolites, *cis*-permethrin and *trans*-permethrin, were detected at levels of 34 and 36 pg/ml in human cord serum, respectively [35]. Permethrin has been shown to alter gene expression and induce breaks in genes associated with leukemia and lymphoma in peripheral blood mononuclear cells exposed *in vitro* [36]. Finally, TCMTB is widely used as a wood preservative, an antimicrobial chemical for water systems, as a preservative for paper products, leather products, paints and wallpaper, and also as a pesticide in seed treatment for barley, cotton, corn, oats, rice and wheat [37]. While data on human intake is scarce, inhalation has been associated with testicular cancer in rodents (TCMTB risk assessment for the reregistration eligibility decision (RED) document, 2006). Importantly, the effects on meiosis from exposures to DBP, permethrin and TCMTB remain poorly understood.

Here we identified a set of chemical exposures affecting the germline and resulting in aneuploidy by using a high-throughput screening strategy in *C. elegans*. Subsequent analysis of three chemicals identified in this screen, DBP, permethrin, and TCMTB, provides new insights into their effects during meiosis and early embryogenesis. Exposure to these chemicals resulted in elevated DNA double-strand break (DSB) formation during meiosis and activation of a DNA damage checkpoint as indicated by elevated phosphorylated CHK-1 (pCHK-1) signal and p53/CEP-1-dependent germ cell apoptosis. Oocytes in diakinesis exhibited defects such as chromosome fragments suggestive of impaired meiotic DSB repair. Live cell imaging revealed chromosome segregation defects and spindle abnormalities during early embryogenesis. Finally, germline-specific expression for conserved DSB formation, repair and DNA damage checkpoint signaling genes is altered following the chemical exposures. These results show that this high-throughput screening platform can be successfully applied to rapidly and reliably identify chemicals affecting germline function and suggest that DBP, permethrin, and TCMTB interfere with maintenance of genomic integrity during meiosis and achieving accurate chromosome segregation.

Results

High-throughput screening of environmental chemicals encompassing phthalates, pesticides, and chemicals used in hydraulic fracturing and crude oil processing

Our high-throughput screening platform takes advantage of two key features of *C. elegans*: their transparency and the rarity of males (X0<0.2% of offspring of self-fertilizing XX

A *Pxol-1::gfp;col-121 (nx3)*

↓ Synchronize by hypochlorite treatment

↓ Grow on NGM plate to L4 stage

↓ Chemical exposure (100 µM) 300 worms/well for 24 hours

↓ COPAS Biosort

GFP $^+$ embryos

GFP $^-$ embryos

B Fold increase over DMSO

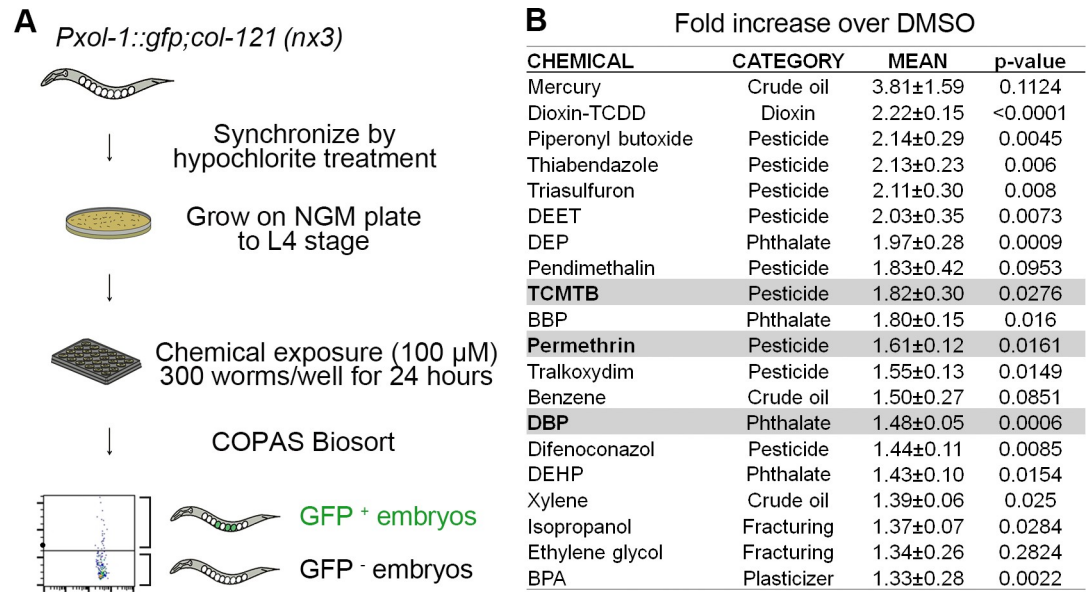| CHEMICAL	CATEGORY	MEAN	p-value
Mercury	Crude oil	3.81±1.59	0.1124
Dioxin-TCDD	Dioxin	2.22±0.15	<0.0001
Piperonyl butoxide	Pesticide	2.14±0.29	0.0045
Thiabendazole	Pesticide	2.13±0.23	0.006
Triasulfuron	Pesticide	2.11±0.30	0.008
DEET	Pesticide	2.03±0.35	0.0073
DEP	Phthalate	1.97±0.28	0.0009
Pendimethalin	Pesticide	1.83±0.42	0.0953
TCMTB	Pesticide	1.82±0.30	0.0276
BBP	Phthalate	1.80±0.15	0.016
Permethrin	Pesticide	1.61±0.12	0.0161
Tralkoxydim	Pesticide	1.55±0.13	0.0149
Benzene	Crude oil	1.50±0.27	0.0851
DBP	Phthalate	1.48±0.05	0.0006
Difenoconazol	Pesticide	1.44±0.11	0.0085
DEHP	Phthalate	1.43±0.10	0.0154
Xylene	Crude oil	1.39±0.06	0.025
Isopropanol	Fracturing	1.37±0.07	0.0284
Ethylene glycol	Fracturing	1.34±0.26	0.2824
BPA	Plasticizer	1.33±0.28	0.0022

Fig 1. Flowchart for high-throughput screening strategy and readout. (A) Worms carrying a collagen gene mutation (*col-121(nx3)*) for increased cuticle permeability and a male-specific promoter driving GFP expression in embryos (*Pxol-1::gfp)*, were synchronized by hypochlorite treatment. Age-matched L1 stage animals were grown on plates (6,000 per 100 mm plate) until reaching the L4 stage. L4 stage animals were dispensed into 24-well plates (300 worms/well) with each well containing OP50 *E. coli* (OD600 = 24) in M9 buffer and a single chemical from our library (≤100 µM each) followed by a 24-hour incubation at 20˚C. After thoroughly washed in M9, young adult animals were sorted based on fluorescence intensity with the COPAS Biosort. Adult worms with GFP$^+$ embryos are detected as distinct from worms carrying GFP$^-$ embryos and debris, which are below the threshold (black horizontal line). Threshold was determined by comparing levels of GFP$^+$ embryos detected in two genetic mutants, *Pxol-1::gfp* and *Pxol-1::gfp;him-8*. More than 5,000 animals were assessed in biological triplicates for each chemical exposure. **(B)** Readouts obtained with the COPAS Biosort for the chemicals that showed higher fold increase in GFP$^+$ embryos compared to DMSO than BPA, a known endocrine disruptor (mean ± SEM; *p*-values calculated by the paired two-tailed *t*-test, 95% C.I.). The three chemicals highlighted in gray, TCTMB, permethrin, and DBP, were assessed further for their effects on germline functions.

hermaphrodites; [38]), to identify chemical exposures that impair chromosome segregation in the germline and result in a high incidence of males. Increased X chromosome nondisjunction is detected using the reporter strain that has GFP expression controlled by a male-specific promoter (*Pxol-1*::GFP) [39,40], and carrying a collagen gene mutation (*col-121(nx3)*) that increases cuticle permeability without affecting the worm's life cycle [41]. The *col-121* collagen gene mutation allows us to reduce the chemical concentrations to ≤100 µM, which are concentrations that circumvent lethality, are frequently used in chemical screens in *C. elegans*, and correlate well with mammalian reproductive endpoints ([42]; Fig 1A and Materials and Methods).

Briefly, we synchronized animals at the L1 larval stage by hypochlorite treatment and placed them on NGM plates with *E. coli* OP50 bacteria for food until the last larval stage (L4). Worms were exposed for 24 hours in 24-well plates starting at the L4 stage, when their gonads are fully formed, in liquid (M9 buffer) with OP50. Importantly, use of live bacteria is not detrimental resulting in low false-positive and–negative rates ([15,42,43]; S1A Fig). Gravid exposed mothers were then screened for increased incidence of GFP$^+$ eggs (destined to become males) by comparison to vehicle alone (0.1% DMSO) using the COPAS Biosort (Union Biometrica), which allows for rapid sorting of live worms based on fluorescent intensities. We screened more than 5,000 animals in triplicate biological repeats for each chemical exposure. The 46 chemicals encompassed pesticides, phthalates, and chemicals used in hydraulic fracturing and

crude oil processing (S1 Table). GFP positive signal above background from each chemical exposure was calculated as fold increase over DMSO (Fig 1B and S1 Table; also see Materials and Methods).

We identified nineteen chemicals showing higher fold increase over DMSO than BPA, an endocrine disruptor shown to affect meiosis leading to increased chromosome nondisjunction in worms and mammals (Fig 1B). Three of these are chemicals used in crude oil processing (mercury, benzene and xylene), with mercury scoring highest from among all chemicals tested. Reprotoxic effects have been previously reported for mercury, benzene and xylene [44,45]. Mercury bioaccumulates and can cause pathophysiological changes in the hypothalamus pituitary gland that may alter follicle-stimulating hormone (FSH) and preovulatory luteinizing hormone (LH) release thereby affecting reproductive function [44]. Women with occupational exposure to the hydrocarbons benzene and xylene have been shown to have reduced LH and mid-luteal phase pregnanediol 3-glucuronide (pd3G) as well as increased follicular-phase pd3G, which can cause reproductive abnormalities [45,46]. Nine of the chemicals were pesticides including thiabendazole, triasulfuron, and pendimethalin, which previous *in vivo* and *in vitro* studies have shown to be genotoxic and can result in mammalian germ cell aneuploidy [15,47–51]. Piperonyl butoxide, another pesticide in the list, has been shown to induce decreased female reproductive organ weight and histopathological changes in the ovary, uterus and vagina in rats likely due to its anti-estrogenic activity [52]. Four were phthalates (DEP, BBP, DBP, and DEHP), which are commonly added as solvents, additives and stabilizers to personal care products and medications and have adverse effects on reproductive and developmental health in humans (reviewed in [53]). Exposure to phthalates has also been shown to disturb sperm function [54,55], increase the percentage of pyriform sperm heads [56], increase DNA damage in sperm [57–60], impair mouse primordial follicle assembly *in vitro* [61] and reduce oocyte quality, embryonic developmental competency as well as alter expression of ovarian and pre-implantation embryonic genes in mice [62]. Finally, epidemiological studies suggest that exposure to isopropanol and ethylene glycol, chemicals used in hydraulic fracturing, may have a negative impact on human reproductive health [63]. The observed increase in X chromosome nondisjunction detected for all of these chemicals suggests effects in germline functions that will require further investigation. For further validation of this high-throughput screening strategy, we selected a phthalate, DBP, and two pesticides, TCMTB and permethrin. These were selected given that they elicited elevated levels of X chromosome nondisjunction and their reprotoxicity is less understood, allowing us to also gain more insight into their effects in germline function (see below).

Exposures to DBP, permethrin, and TCMTB result in increased embryonic lethality and altered germline chromosome morphogenesis

To assess whether DBP, permethrin and TCMTB affect chromosome segregation in general (including autosomes), and determine the dose of exposure for subsequent studies, we exposed worms to various concentrations of these chemicals (1, 10, 100 and 500 μM) for 24 hours starting at late L4, as in the high-throughput screen, and scored the number of eggs laid (brood size), embryonic lethality, and larval lethality. A decreased brood size and increased embryonic lethality can be due in part to defects during meiosis leading to errors in autosomal chromosome segregation and the consequent formation of aneuploid gametes in *C. elegans* [9,38,64]. We observed approximately a 50% reduction in the mean numbers of eggs laid on plates, which is indicative of increased sterility, for worms exposed to 500 μM DBP, 500 μM permethrin and both 100 μM and 500 μM TCMTB, compared to vehicle alone (Fig 2A). We also observed significantly increased embryonic lethality for exposures starting at 100 μM for DBP
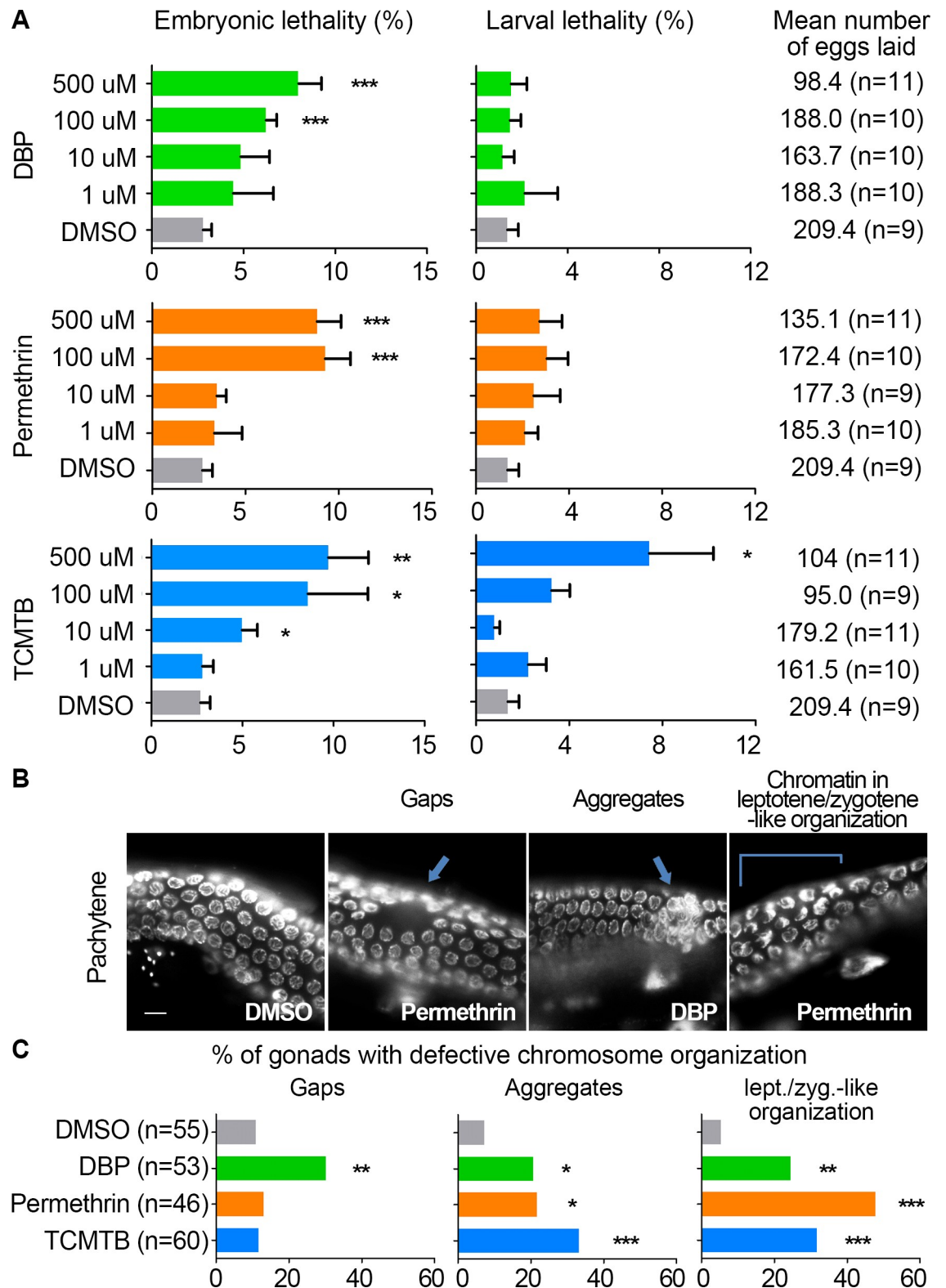
A

B

C

Fig 2. DBP, Permethrin, and TCMTB exposures result in increased embryonic lethality, sterility and defects in chromosomal organization in the germline. **(A)** Plate phenotypes for indicated chemical exposures. Embryonic lethality, larval lethality and the number of eggs laid (brood size) are shown for the indicated doses of exposures and compared to vehicle alone (0.1% DMSO). Error bars represent SEM. *P<0.05, **P<0.01, and ***P<0.001 by the two-tailed Mann-Whitney test, 95% C.I. **(B)** Images show pachytene

nuclei in the germlines of whole, undissected worms fixed with Carnoy's fixative and stained with DAPI that were exposed to vehicle control, 100 μM DBP, 100 μM permethrin, and 10 μM TCMTB. Chemical exposures lead to increased numbers of gonads with gaps (discontinuities or spaces lacking germ cell nuclei; arrow in second panel), aggregated nuclei (arrow, third panel) and DAPI-bright nuclei with chromosomes collapsed to one side (area indicated with a bracket, fourth panel) instead of dispersed throughout the nuclear periphery and organized in clear parallel tracks as seen in control at that stage. Scale bar, 5 μm. **(C)** Percentage of gonads exhibiting gaps, aggregates, or nuclei with chromatin in a leptotene/zygotene-like organization, in pachytene (n = number of gonads examined). * $P < 0.05$, ** $P < 0.01$, and ** $P < 0.001$ by the two-sided Fisher's exact test.

and permethrin ($P < 0.001$; two-tailed Mann-Whitney test, C.I. 95%) and 10 μM for TCMTB ($P < 0.05$) (Fig 2A). Furthermore, we observed higher larval lethality among the progeny of worms exposed to 500 μM TCMTB ($P < 0.05$). These data further support and extend the results of our high-throughput screen suggesting that all three chemicals affect chromosome segregation in general and not limited to the X chromosome. Moreover, based on this analysis, doses of 100 μM for DBP and permethrin, and 10 μM for TCMTB, which result in embryonic lethality without significantly reducing the brood size or causing larval lethality, were used for all subsequent analysis.

To determine whether the increased chromosome nondisjunction is due in part to defects during meiosis, we examined DAPI-stained gonads from worms following exposures. In *C. elegans*, nuclei are positioned in a spatial and temporal gradient along the germline facilitating the identification of alterations in chromosome organization at specific meiotic stages [9]. We observed an increase in the number of gonads with gaps (areas with a reduced density of nuclei) in worms exposed to DBP compared to vehicle alone (30.2%, n = 53, and 10.9%, n = 55, respectively), as well as the presence of nuclei with DAPI-bright chromatin forming aggregates and nuclei with DAPI-bright and collapsed chromatin in a leptotene/zygotene-like organization at late pachytene in the gonads of worms exposed to all three chemicals compared to vehicle (aggregates: DBP: 20.8%, n = 53; permethrin: 21.7%, n = 46; TCMTB: 33.3%, n = 60; and DMSO: 7.3%, n = 55; leptotene/zygotene-like organization: DBP: 24.5%, n = 53; permethrin: 47.8%, n = 46; TCMTB: 31.7%, n = 60; and DMSO: 5.5%, n = 55) (Fig 2B and 2C). However, these defects are not due to overt impairments to early stages of meiotic progression or chromosome synapsis (S2A–S2E Fig). This is evidenced by normal localization of phosphorylated SUN-1 (SUN-1 S8), where SUN-1 corresponds to a conserved inner nuclear envelope protein with CHK-2- and PLK-2-dependent phosphorylation, with a signal appearing upon entrance into meiosis at the leptotene/zygotene stage and persisting on nuclei until mid-pachytene [65]. This is further supported by the normal localization of SYP-1, a structural component of the central region of the synaptonemal complex, observed associating with nuclei upon entrance into meiosis, forming full tracks between homologs at pachytene and starting to disassemble by late pachytene [66]. Taken together, these results show evidence of sterility, embryonic lethality and larval lethality as well as chromosome defects during pachytene after DBP, permethrin and TCMTB exposure, but these are not due to defects in meiotic progression or chromosome synapsis.

DBP, permethrin, and TCMTB exposures result in increased germ cell apoptosis, elevated levels of meiotic DSBs and altered meiotic DSB repair

Nuclei with DAPI-bright and collapsed chromatin at late pachytene have been previously correlated with germ cells undergoing apoptosis [67]. To determine whether the chemical exposures are causing increased germ cell apoptosis, we scored germline nuclei undergoing apoptosis (germ cell corpses, also referred to as apoptotic bodies) by acridine orange staining as in [39]. In wild type, animals exhibit less than three apoptotic bodies in late pachytene reflecting regular physiological apoptosis [64,68] (Fig 3A). We observed a significant 2- to 3-fold increase in the levels of germ cell corpses in late pachytene following all three chemical
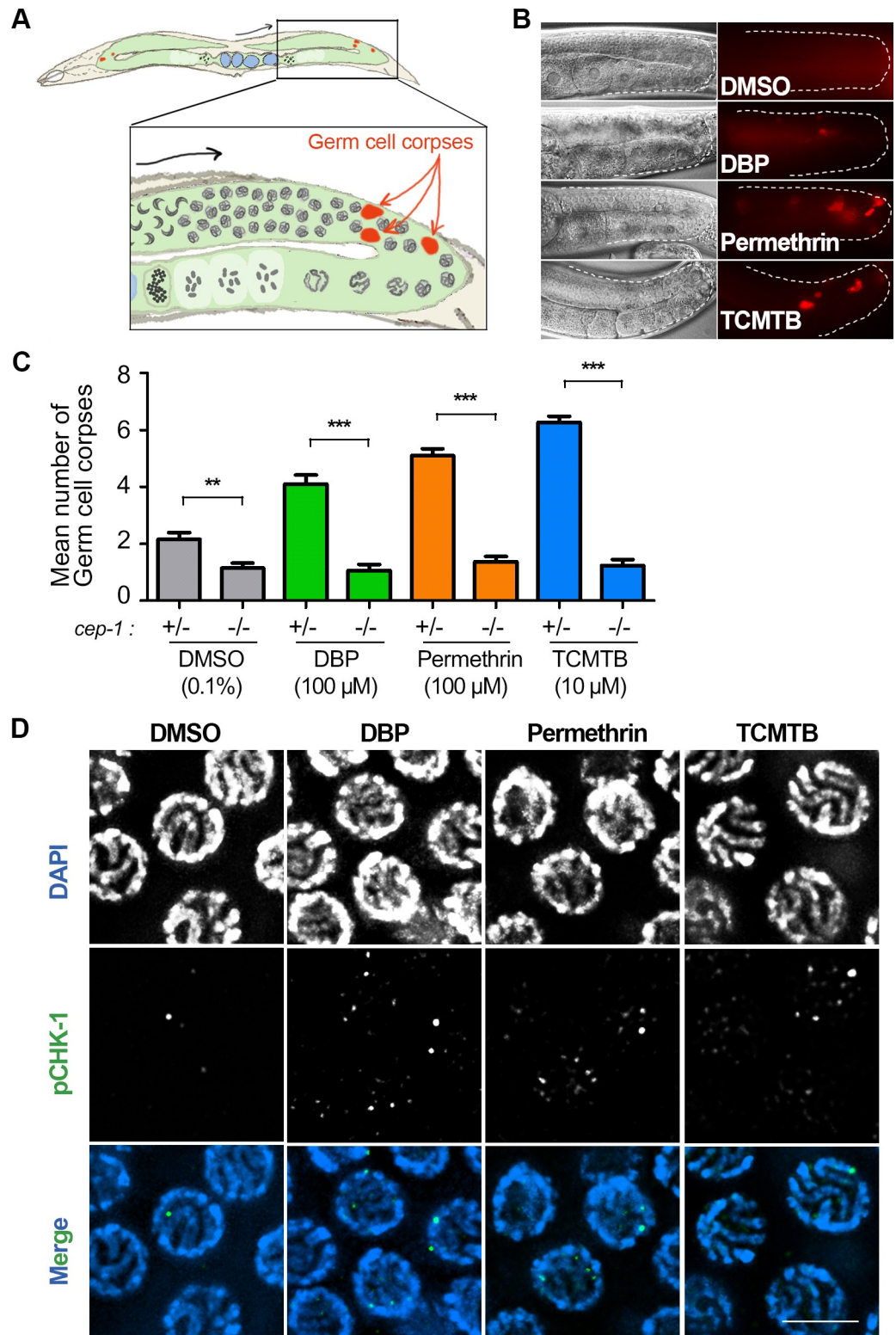
Fig 3. DBP, Permethrin, and TCMTB exposures lead to p53/CEP-1-dependent increased germ cell apoptosis and CHK-1 activation. (A) Schematic representation of *C. elegans* and the area where DNA damage checkpoint activation of germ cell apoptosis is detected in the germline. Inset represents zoom-in of one gonad arm. Black arrow indicates orientation of progression through meiosis while red arrows indicate germ cell corpses (red) observed at late pachytene near the gonad bend. **(B)** Chemical exposures caused a significant increase in the number of germ cell corpses observed at late pachytene compared to vehicle alone. Gonads are traced to facilitate visualization. On the left is the Nomarski optics

view and to the right are the acridine orange stained germ cell corpses (red). **(C)** Graphical representation showing mean number of germ cell corpses detected for each indicated chemical. Levels of germ cell corpses were significantly reduced in a p53/*cep-1*-dependent manner. Note that basal level of toxicity for DMSO, as previously described [42,103], is also reduced in a *cep-1* mutant background. Analysis was done for three independent biological repeats. More than 30 gonads were scored for each chemical. Error bars represent SEM. **P<0.01, ***P<0.0001 by the two-tailed Mann-Whitney test, 95% C.I. **(D)** High-resolution images of mid to late pachytene nuclei from whole-mounted gonads immunostained for phospho CHK-1 (pCHK-1; green) and co-stained with DAPI (blue). Elevated levels of pCHK-1 were observed in chemical-treated worms compared to control. Scale bar, 5 μm.

exposures compared to vehicle alone (Fig 3B and 3C). Moreover, the elevated germ cell apoptosis was observed in a dose-dependent manner, starting at 100 μM for DBP and permethrin, and 10 μM for TCMTB (S3 Fig). In *C. elegans*, physiological germ cell apoptosis does not depend on p53/CEP-1, which responds to genotoxic stress as a result of the activation of a DNA damage checkpoint [69]. Analysis of germ cell apoptosis levels in *cep-1;col-121* worms revealed the elevated apoptosis following all three chemical exposures was p53/CEP-1-dependent (Fig 3C). Activation of a DNA damage checkpoint was further supported by the increased signal detected in pachytene nuclei for a checkpoint kinase involved in DNA damage sensing, phosphorylated CHK-1 [70], following each chemical exposure (Fig 3D). Therefore, DBP, permethrin, and TCMTB exposures lead to activation of a DNA damage checkpoint resulting in increased p53/CEP-1-dependent germ cell apoptosis to clear affected nuclei.

The pachytene DNA damage checkpoint can be activated by the presence of unrepaired DSBs or aberrant recombination intermediates [64]. To examine this further, we quantified levels of RAD-51 foci as in [67]. RAD-51 binds to 3' ssDNA ends at DSBs to promote strand invasion/exchange during DSB repair [71]. In vehicle-exposed gonads, like in wild type, low levels of RAD-51 foci were observed in nuclei at the premeiotic tip (zones 1–2) undergoing mitosis, as well as upon entrance into meiosis at transition zone where leptotene/zygotene stage nuclei are located (zone 3). Levels continued to rise throughout pachytene, peaking by mid-pachytene (zone 5), and then decreased by late pachytene (zone 7) as DSB repair progressed (Fig 4A–4C). In contrast, levels of RAD-51 foci were elevated specifically during meiosis for all three chemical exposures (Fig 4B and 4C). Levels of RAD-51 foci were indistinguishable from vehicle alone throughout the mitotic zone, but were higher than vehicle alone during pachytene. Moreover, analysis of *col-121* worms depleted of SPO-11, the protein required for meiotic DSB formation, further confirmed that the elevated levels of RAD-51 foci were SPO-11-dependent and therefore, meiotic-specific and not due to damage from the chemicals to the chromosomes (S4A–S4D Fig).

To determine whether the elevated levels of RAD-51 foci may be due in part to elevated DSB levels, we quantified RAD-51 foci in *rad-54;col-121* double mutants following chemical exposures. In a *rad-54* mutant, DSBs are formed and RAD-51 associates with DSB repair sites, but further repair is blocked essentially "trapping" DSB-bound RAD-51 and allowing for quantification of the total number of DSBs [72]. Levels of RAD-51 foci were significantly higher during meiosis for all three exposures compared to vehicle alone (Fig 4D). Taken together, these results suggest that exposures to DBP, permethrin and TCMTB result in elevated meiotic DSB levels and impaired DSB repair leading to activation of a DNA damage checkpoint and p53-dependent increased germ cell apoptosis.

Chemical exposures lead to defects in late prophase I and first embryonic cell division

To determine whether exposures to DBP, permethrin and TCMTB might also result in defects at late prophase I, we examined chromosome morphology in oocytes at late diakinesis. In *C.*
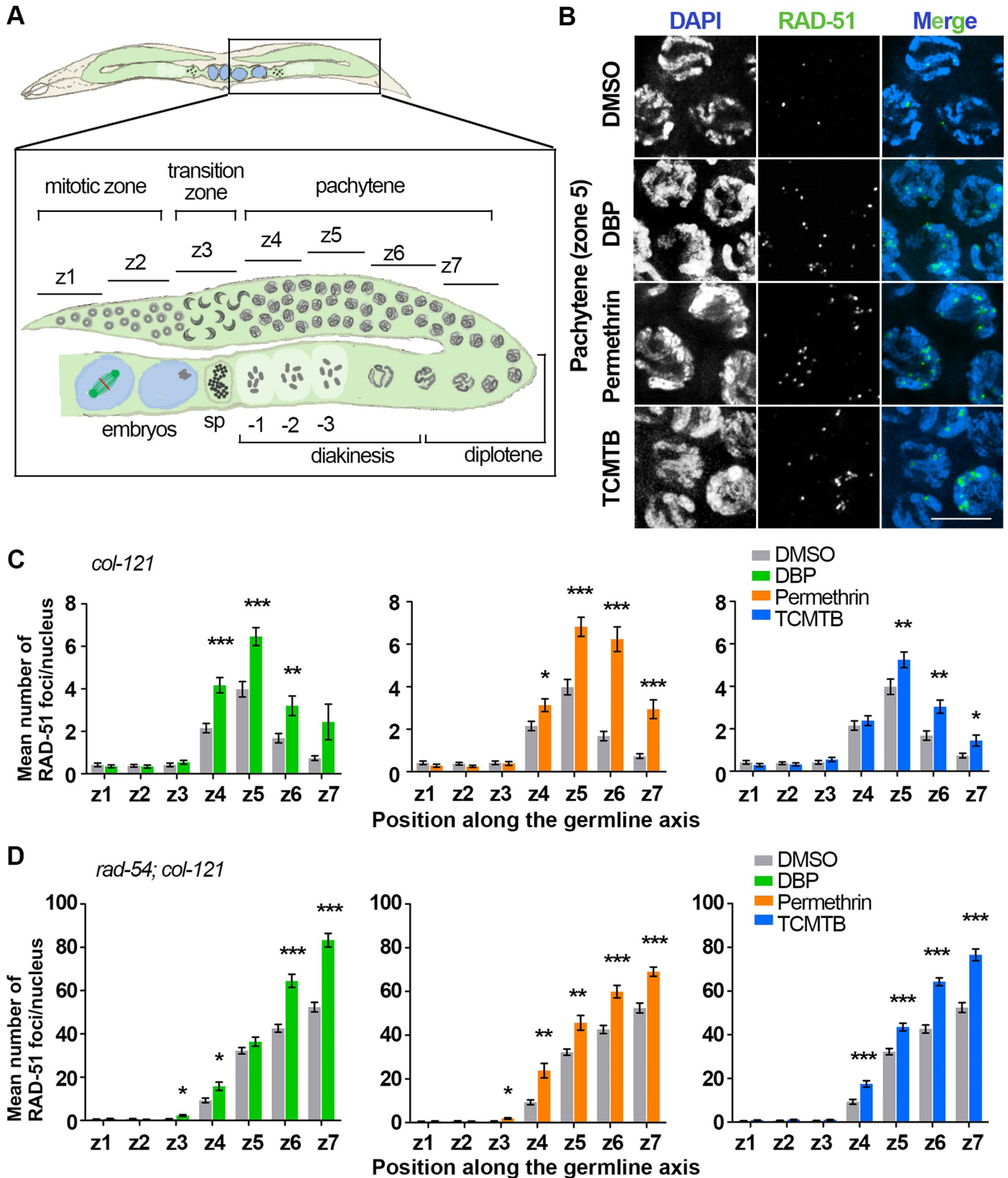
Fig 4. Chemical exposures result in increased DSB formation and impaired DSB repair. (A) Schematic representation of a *C. elegans* germline indicating the position of the equally sized zones (z1-z7) scored for RAD-51 foci. Nuclei in z1 and z2 are undergoing mitosis. They enter meiosis at z3 when they enter the transition zone, which corresponds to the leptotene/zygotene stages. Nuclei then proceed through pachytene (z4-z7), diplotene and diakinesis on their way into the

uterus. sp: spermatheca. -1 indicates the oocyte closest to the spermatheca. **(B)** Representative images of pachytene nuclei (z5) immunostained for RAD-51 (green) and co-stained with DAPI (blue). Levels of RAD-51 foci in pachytene nuclei are elevated for each chemical exposure compared with control. Note that chromosomes in pachytene nuclei still exhibit a leptotene/zygotene-like organization in the cases of DBP and permethrin exposures. Scale bar, 5 μm. **(C)** Histograms show the mean number of RAD-51 foci scored per nucleus for each zone from *col-121* worms. Elevated levels of foci are observed persisting until late pachytene indicating a defect in DSB repair. >5 gonads from three independent biological repeats were scored for each indicated exposure. Error bars represent SEM. **(D)** Quantification of the mean number of RAD-51 foci scored per nucleus in *rad-54;col-121* worms. DSB levels were significantly higher upon the chemical exposures compared to vehicle alone. 3 gonads were scored for each chemical from two independent biological repeats. Error bars represent SEM. *P<0.05, **P<0.01, ***P<0.001 by the two-tailed Mann-Whitney test, 95% C.I.

https://doi.org/10.1371/journal.pgen.1007975.g004

elegans, the six pairs of attached homologs (bivalents) are detected as six DAPI-stained bodies during diakinesis (Fig 5B). With high resolution microscopy we analyzed the -1 and -2 oocytes at diakinesis, which correspond to the two last oocytes proximal to the spermatheca (Fig 4A). We observed increased numbers of oocytes carrying chromosomes exhibiting a frayed morphology, chromatin bridges and chromosome fragments in germlines exposed to all three chemicals compared to vehicle alone (Fig 5A and 5B). This suggests that despite activation of p53-dependent apoptosis in late pachytene, some nuclei that failed to undergo normal DSB repair are progressing into late diakinesis.

To determine if DBP, permethrin and TCMTB exposures also impact early embryogenesis, we examined the first embryonic cell division by live imaging using transgenic worms carrying H2B::mCherry; γ-tubulin::GFP and the *col-121(nx3)* mutation. We detected the presence of lagging chromosomes (congression failure) and spindle abnormalities in the embryos examined from all three chemical exposures, and evidence of chromatin bridges in the metaphase to anaphase transition from DBP and TCMTB exposures compared to vehicle alone (Fig 5C and 5D). These results suggest that these chemical exposures affect meiosis as well as early embryogenesis, supporting the elevated chromosome nondisjunction detected by high-throughput screening following these treatments.

Chemical exposures cause altered germline gene expression

Given the effects on DSB formation, repair and DNA damage checkpoint activation observed during meiosis following all three chemical exposures, we next examined whether these defects arise from alterations in expression of DSB repair and DNA damage response genes. We examined mRNA levels by quantitative RT-PCR for 15 critical and conserved genes involved in these processes (Fig 6A and 6B). We used *glp-1;col-121* double mutants that develop as wild type at 15˚C, but grow into adults lacking a germline when shifted to 25˚C [73], to distinguish changes in gene expression occurring in the soma from those taking place in the germline. All three chemical exposures led to a significant increase in *chk-1* expression at 15˚C (P<0.05), but not at 25˚C (Fig 6A and 6B), indicating a germline-specific change in gene expression and correlating with the increased pCHK-1 foci we detected in the germline (Fig 3D). Moreover, DBP exposure resulted in germline-specific up regulation of *spo-11* and down regulation of *mre-11* (P<0.001 and P<0.05, respectively), which are factors involved in DSB formation and repair, as well as upregulation of *prmt-5* (P<0.01), involved in regulation of DNA damage-induced apoptosis [74,75]. Taken together, these results suggest that germline-specific alterations in the expression of genes involved in DSB formation, repair and response may contribute in part to the defects in maintaining genomic integrity and achieving accurate chromosome segregation observed in the germline following these chemical exposures.

Discussion

We showed that a high-throughput screening strategy can be successfully applied to identify environmental chemicals causing aneuploidy using the nematode *C. elegans*. Due to the
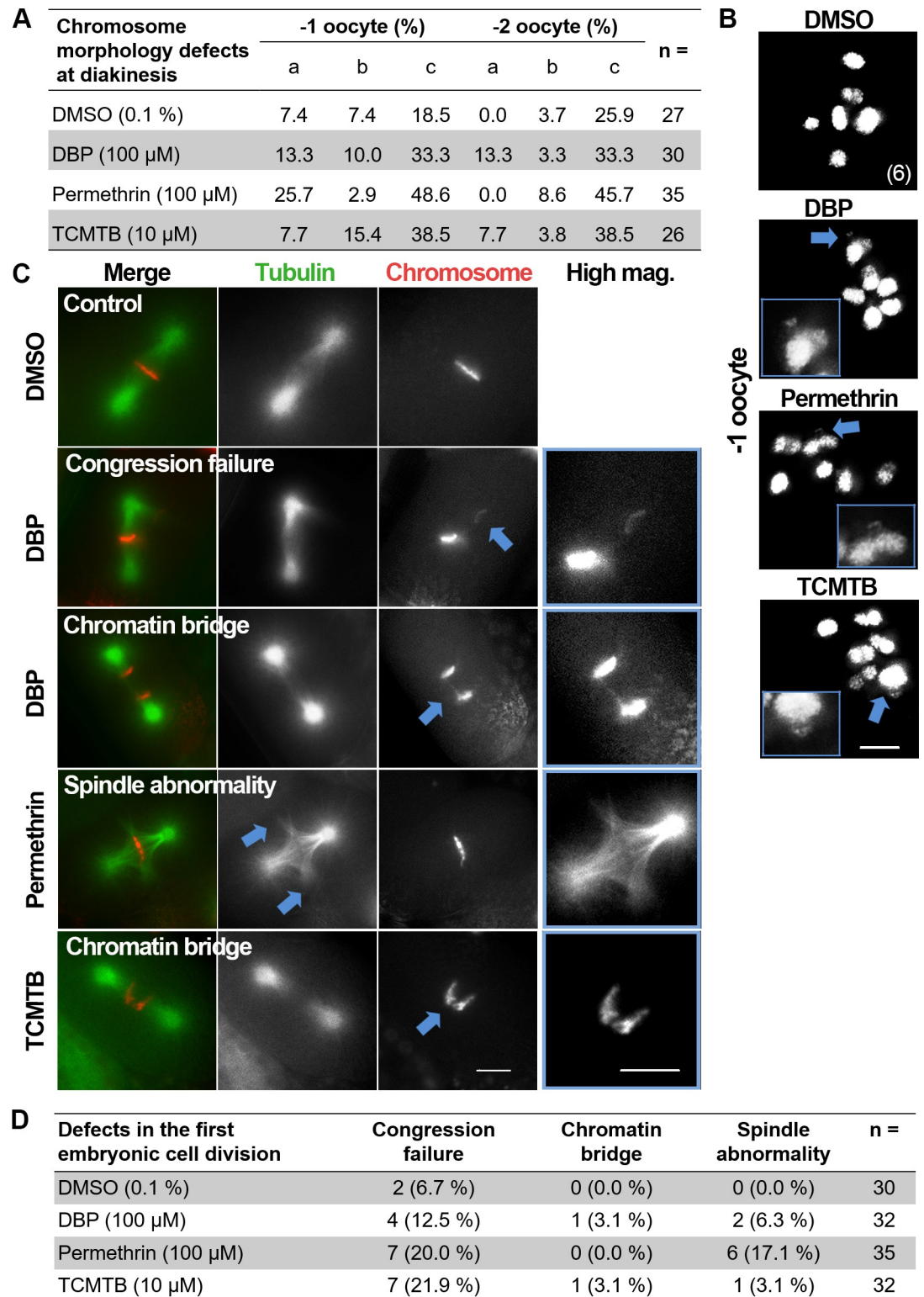
A

Chromosome morphology defects at diakinesis	-1 oocyte (%)			-2 oocyte (%)			n =
	a	b	c	a	b	c	
DMSO (0.1 %)	7.4	7.4	18.5	0.0	3.7	25.9	27
DBP (100 μM)	13.3	10.0	33.3	13.3	3.3	33.3	30
Permethrin (100 μM)	25.7	2.9	48.6	0.0	8.6	45.7	35
TCMTB (10 μM)	7.7	15.4	38.5	7.7	3.8	38.5	26

B

C

D

Defects in the first embryonic cell division	Congression failure	Chromatin bridge	Spindle abnormality	n =
DMSO (0.1 %)	2 (6.7 %)	0 (0.0 %)	0 (0.0 %)	30
DBP (100 μM)	4 (12.5 %)	1 (3.1 %)	2 (6.3 %)	32
Permethrin (100 μM)	7 (20.0 %)	0 (0.0 %)	6 (17.1 %)	35
TCMTB (10 μM)	7 (21.9 %)	1 (3.1 %)	1 (3.1 %)	32

Fig 5. Chemical exposures lead to defects at diakinesis and the first embryonic cell division. (A) Quantification of the chromosome morphology defects observed in diakinesis (-1 and -2 oocytes). a: chromosome fragments, b: chromatin bridges, c: frayed chromosomes, n = total number of oocytes scored. **(B)** High resolution images of oocytes at diakinesis positioned right before the spermatheca (-1 oocyte). Six intact bivalents are observed in control. In contrast, frayed chromosomes, chromosome fragments and chromosome bridges (arrows and magnified in insets) are observed at higher levels in the germlines of chemical-

exposed worms. Scale bar, 5 μm. **(C)** Representative images from time-lapse analysis of the first embryonic division in vehicle alone and DBP-, permethrin- and TCMTB-exposed H2B::mCherry; γ-tubulin::GFP; *col-121(nx3)* worms. A normal metaphase I configuration is shown for vehicle alone. Arrows and insets show examples of chromosomes that fail to align at the metaphase plate, chromatin bridges at the metaphase to anaphase transition and spindle abnormalities observed following exposures to all three chemicals. Scale bars, 5 μm. **(D)** Quantification of the time-lapse analysis of the first embryonic division. n = total number of embryos scored.

increasing number of chemicals being introduced into the environment and their broad uses, strategies for rapidly assessing toxicity, in a manner predictive of their effects on human health, are in high demand. *C. elegans* is a metazoan system that offers various advantages for this type
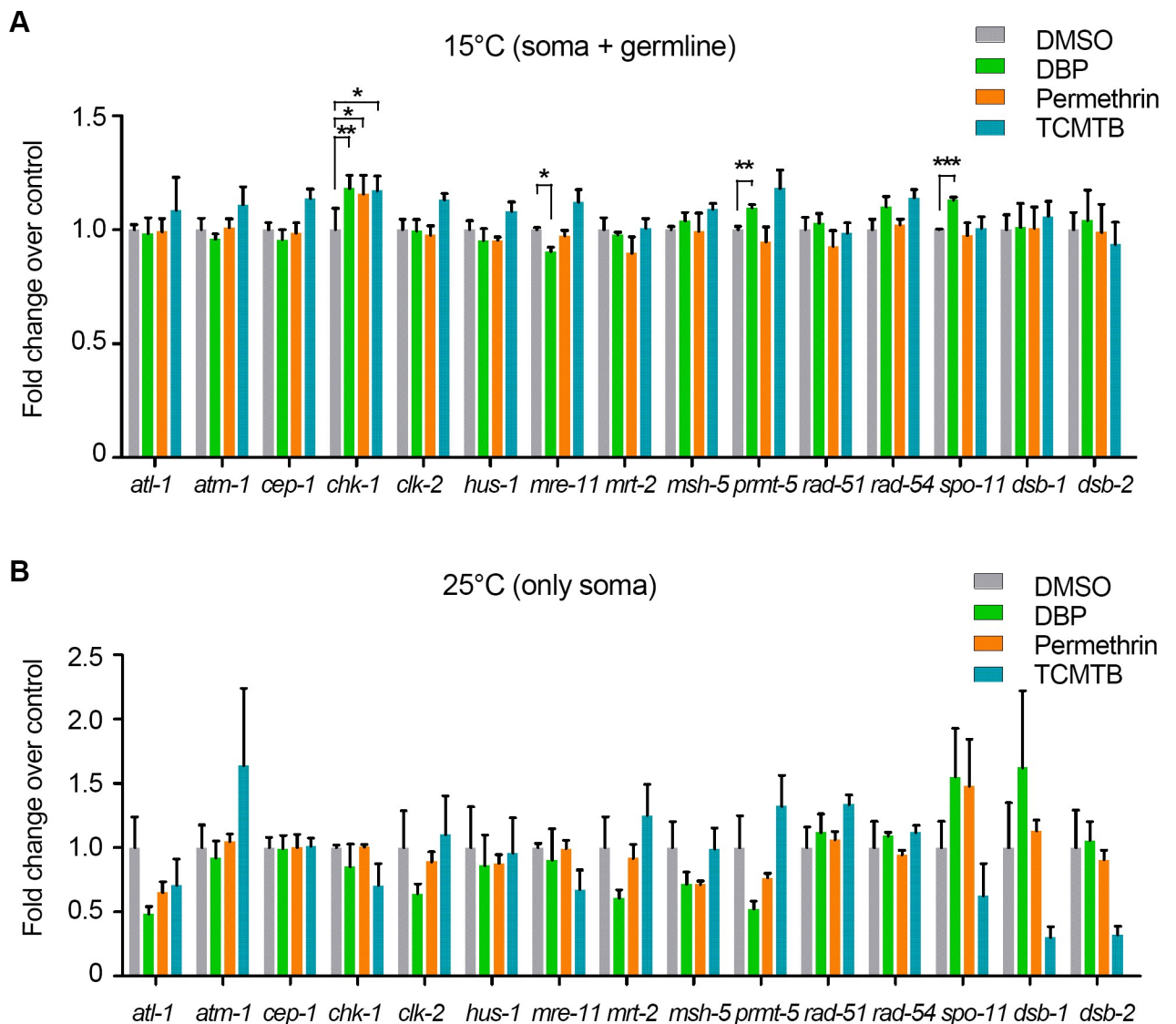

Fig 6. Germline-specific gene expression of DSB formation, repair and response genes is altered by chemical exposures. Expression levels of a panel of genes responsible for DSB formation, repair and DNA damage response were examined by quantitative RT-PCR in *glp-1(bn18);col-121(nx3)* worms that grow without a germline when shifted from 15°C **(A)** to 25°C **(B)**. Thus, 15°C represents gene expression in both soma and germline, while 25°C represents expression only in the soma. The expression levels of 15 critical and conserved genes were measured from either three (15°C) or four (25°C) independent biological replicates (each performed with technical triplicates) and normalized to *gpd-1* (GAPDH). Y-axis indicates gene expression level change relative to vehicle alone. Error bars represent SEM. *P<0.05, **P<0.01, ***P<0.001 by the unpaired two-tailed *t*-test.

of analysis including low maintenance costs, a rapid life cycle and a high degree of conservation of its genes and biochemical pathways with humans [9,76–80]. This nematode is also being successfully used in high-throughput screens of compounds and genes impacting pathways related to human disease [11,13,81–83]. *C. elegans* is also an ideal model system specifically for studying the effects of chemical exposures on the germline since genes and pathways involved in regulating key processes such as germ stem cell renewal and differentiation, meiosis, ovulation and embryogenesis are conserved between *C. elegans* and humans. Moreover, its germline is well characterized and amenable to studies using genetic, biochemical, and molecular biology tools combined with powerful cytological approaches [8,12,14]. Our high-throughput screen identified several different classes of chemicals that are leading to increased chromosome nondisjunction and follow up studies will further explore how they are affecting the germline. Along those lines, here we also provided new insights into the effects of DBP, permethrin and TCMTB on germline functions.

DBP is metabolized by esterases to form mono-n-butyl phthalate (mBP) once it enters the body, while permethrin undergoes hydrolysis and oxidation in the liver by carboxylesterases and cytochrome P450 to conjugated and unconjugated *cis/trans* 3-(2,2-dichlorovinyl)-2,2-dimethylcyclopropane carboxylic acid (CVA) with their plasma levels reaching peak values in 5–7 hours [84–86], and TCMTB is converted into cyanide, 2-mercaptobenzothiazole (2-MBT) by cytochrome P450 in the liver [87]. In our study, we exposed worms for 24 hours to 100 µM or 27.8 µg/ml of DBP, which our dose-response studies showed impaired chromosome segregation with low overall toxicity, as determined by both growth and behavior of the worms. Measurement of the internal concentration from whole worm extracts by isotopic dilution mass spectrometric analysis revealed internal levels of 8.9 µg/ml for DBP, and 2.2 µg/ml for mBP, confirming that this chemical reaches internal circulation (Fig 7). A study of a small group of women undergoing IVF in the USA detected a median value of 1.46 ng/ml of mBP in follicular fluid [88] while a larger study of 110 women undergoing IVF in China detected median values for mBP of 2.05 ng/ml in follicular fluid and 102.30 ng/ml in urine and maximum values for DBP of 415 ng/ml in follicular fluid and 2.32 µg/ml in urine [89]. Studies showing the relationship between prenatal phthalate exposure and anogenital distance (AGD) as an outcome of reproductive toxicity detected geometric means for mBP of 67.62 ng/ml in urine from 196 women in Sweden and 15.04 ng/ml in urine from 380 women in the USA [29,90]. This suggests that the levels which resulted in germline defects in *C. elegans* are within the range relevant to human exposures. In this study, worms were exposed for 24 hours to external doses of 100 µM permethrin and 10 µM TCMTB, corresponding to 39.13 µg/ml and 2.38 µg/ml, respectively. Measurement of the internal concentrations from whole worm extracts revealed internal levels of 5.6 µg/ml for *cis-* and *trans*-permethrin combined, and 0.5 µg/ml for 2-methylthio benzothiazole (2-MeS BTH), showing that these chemicals also reach internal circulation (Fig 7). TCMTB is apparently metabolized very rapidly in worms (akin to mammals [87]) and we were unable to detect it in our extracts. We also did not detect either benzothiazole (BTH) or 2-hydroxy benzothiazole (2-OH BTH) metabolites. Unfortunately, data on the concentrations of these metabolites in non-blood tissue or organs in either mammalian models or humans is scarce to nonexistent, thus limiting comparisons regarding exposure levels. However, the internal levels detected for DBP and mBP, coupled with the effects on germline functions detected by our high-throughput screen and follow up studies for all three chemicals, suggest that *C. elegans* offers the necessary sensitivity to detect effects at environmentally relevant doses of exposure.

Here we showed that all three chemicals resulted in elevated meiotic DSB levels, impaired DSB repair, activation of p53-dependent germ cell apoptosis and elevated phosphorylated CHK-1 signal during late pachytene, along with chromosomal abnormalities in oocytes at late
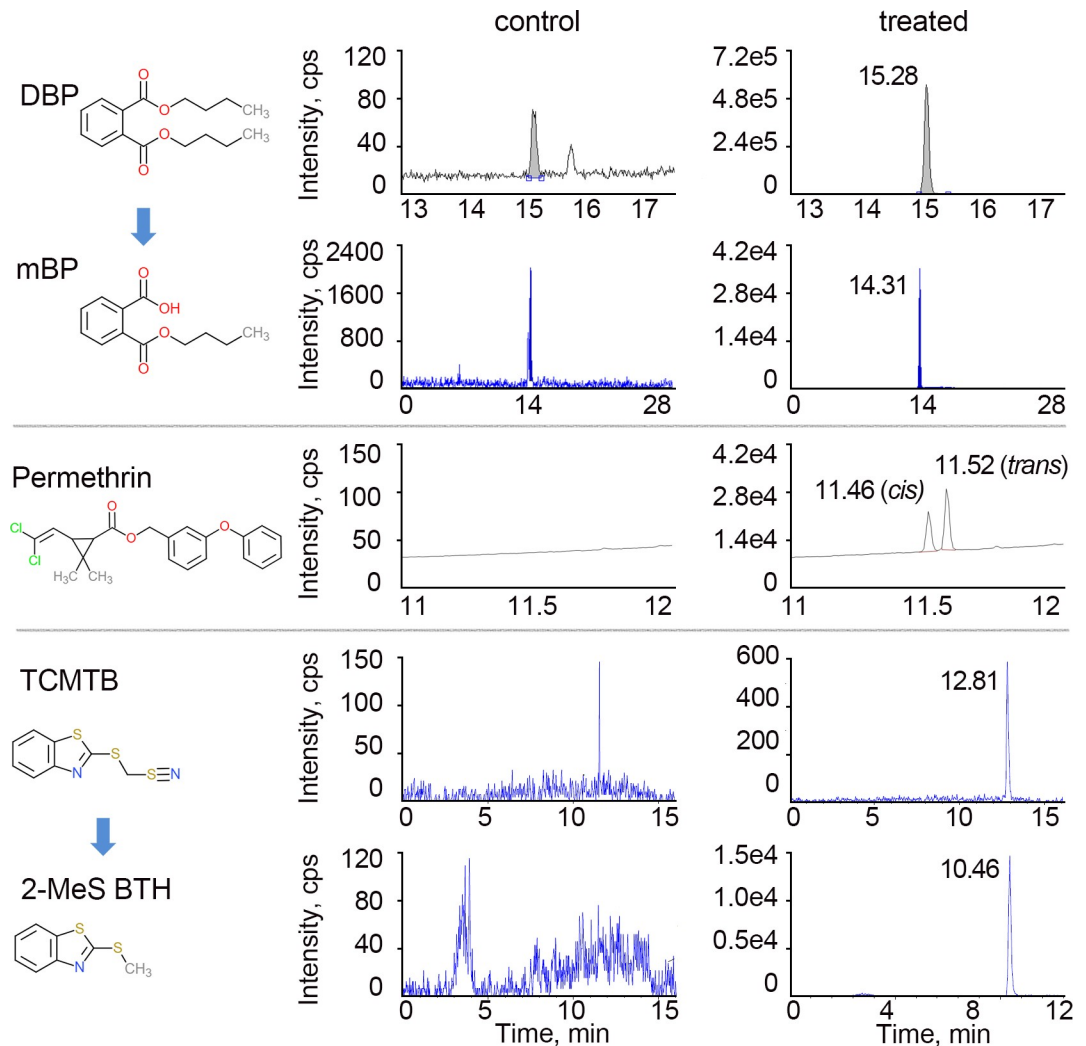
Fig 7. Structures and representative LC-MS/MS and GC-MS chromatograms for DBP, permethrin, TCMTB and their metabolites. Chromatograms on the left show results from the analysis of the indicated chemicals and metabolites in worms exposed to vehicle alone (DMSO; control) and chromatograms on the right show results from worms exposed to DBP, permethrin, and TCMTB (treated). These chemicals were unambiguously identified and quantified using their respective internal standards. Y-axis represents relative abundance of signal intensity and X-axis represents retention time in minutes. The detected concentrations following chemical treatments (right) were consistently greater than in control (note differences in Y-axis). Note that the peak at 12.81 minutes does not correspond to TCMTB (expected peak for TCMTB is at 8.76), suggesting that TCMTB is very rapidly metabolized in the worm.

https://doi.org/10.1371/journal.pgen.1007975.g007

diakinesis and impaired chromosome segregation during early embryogenesis. *In vitro* studies of the effects of DBP exposure on Sertoli cell culture showed increased apoptosis stemming from inhibiting the PI3K/AKT and mTOR pathways which promote the proliferation and survival of sperm and the maintenance of testicular homeostasis [26]. Antral follicles isolated from female mice and exposed to DBP exhibited increased expression of the cyclin-dependent kinase inhibitors *Cdkn1a* and *Cdkn2a* and pro-apoptotic factors *Bax* and *Bid* along with down regulation of cyclin *Ccnd2* resulting in growth inhibition and follicular death [28]. Permethrin has been shown to cause DNA damage in mitotic cells where exposure of peripheral blood mononuclear cells (PBMCs) induced breaks in the *KMT2A* and *IGH* genes which can be driver mutations for lymphoma and leukemia along with increased aneuploidy [36]. TCMTB has

been reported as exhibiting relatively low toxicity upon either oral or dermal uptake since it is rapidly metabolized into 2-MBT in the body and excreted through the urinary tract, however it has been considered highly toxic via the inhalation route and resulted in increased incidence of testicular interstitial cell adenomas in male rats [87], (TCMTB risk assessment for the reregistration eligibility decision (RED) document, 2006).

To our knowledge, the germline-specific upregulation of *chk-1* following exposures to DBP, permethrin and TCMTB, and the downregulation of *mre-11* along with the upregulation of *spo-11* and *prmt-5* following DBP exposure, have not been previously reported. This altered gene expression profile is congruent with the elevated meiotic DSB formation, altered meiotic DSB repair and activation of a DNA damage checkpoint observed during meiosis. SPO-11 is the topoisomerase-like conserved protein that catalyzes meiotic DSBs so that the elevated levels of DSB formation observed in DBP exposed worms may be due in part to deregulation of *spo-11* expression. *prmt-5* encodes for the ortholog of human PRMT5, a protein arginine methyl-transferase involved in the post-translational modification of a variety of proteins including histones and G protein-coupled receptors, thereby regulating transcription and signaling [91]. Interestingly, PRMT5 has been proposed to regulate the target gene specificity of p53 in mammals [74] and to negatively regulate apoptotic signaling in response to DNA damage in *C. elegans* by repressing p53/CEP-1 transcriptional activity through downregulation of *cbp-1*/p300, which encodes for a cofactor of CEP-1 [75]. Alternatively, upregulation of *prmt-5* may result in alterations in transcription or chromatin accessibility, for example via its role in histone regulation, which in turn could also contribute to elevated DSB formation and/or altered repair. Finally, *mre-11* encodes for a member of the MRX/N (Mre11, Rad50, Xrs2/Nbs1) complex required for meiotic DSB formation and resection [92–97]. The elevated levels of DSBs and RAD-51 foci detected following DBP exposure suggest that downregulation of *mre-11* may not be interfering with DSB formation and/or end resection in this case. Finally, although all three chemical exposures led to elevated germline-specific *chk-1* gene expression, additional studies will be required to determine how permethrin and TCMTB affect DSB formation and repair during meiosis.

Taken together, our results demonstrate that a high-throughput screening platform can be used in *C. elegans* to successfully identify environmental chemicals affecting the germline. Moreover, our findings revealed the effects of DBP, permethrin, and TCMTB exposures on the germline and potential mechanisms by which DBP affects germline functions, broadening our understanding of the potential effects of environmental toxicants on human reproductive health.

Materials and methods

C. elegans strains

C. elegans strains were cultured at 20˚C under standard conditions as described in [98]. The following mutations and chromosome rearrangements were used in this study: LGI, *cep-1 (lg12501)*, *rad-54(ok615)*; LGIII, *glp-1(bn18)*; LGIV, *col-121(nx3)*, *him-8(e1489)*; LGV, *yIs34* [*Pxol-1::GFP*, *rol-6*].

Calibration of COPAS Biosort parameters and gating of adult population

To ensure the GFP signals detected in the COPAS Biosort stemmed only from gravid worms and not debris, we first synchronized worms at the L1 stage by hypochlorite treatment as in [99] and sorted either *Pxol-1::gfp; col-121* or *Pxol-1::gfp; col-121; him-8(e1489)* worms at different developmental stages (L1 through young adults). Presence of the *him-8* mutation results in a high incidence of male progeny (36.7%; [38]) due to increased X chromosome

nondisjunction. The use of both strains allowed us to exclusively gate adult worms and establish the threshold for worms carrying GFP+ embryos above background. Thus, only an adult population from age-matched animals underwent screening (S1B–S1D Fig).

Chemical exposure and screening with the COPAS Biosort

Age-matched embryos were obtained from gravid worms following sodium hypochloride treatment and subjected to overnight starvation [99]. Thoroughly washed age-matched L1-stage worms were grown on regular NGM plates up to the L4 stage (5,000 to 6,000 L1 worms were grown on each 100 mm plate). Between twenty to thirty thousand L4-stage animals were resuspended in M9 buffer with freshly cultured OP50 bacteria (OD600 = 24). 300 worms in 250 µl of M9 with OP50 bacteria were dispensed, along with each chemical, into individual wells in 24-well plates. All chemicals, except TCDD, were purchased from Sigma Aldrich (St. Louis, MO) and dissolved in DMSO at 0.1 M except for polyacrylamide and hydroxyethyl cellulose, which were dissolved in water respectively at 20 mg/ml and 33 mg/ml for solubility reasons. TCDD was purchased from AccuStandard (New Haven, CT). Final DMSO and chemical concentrations were 0.1% and 100 µM, respectively, except for dicofol, mancozeb, parathion-methyl, phosalone, pyridaben, TCMTB, arsenic oxide, and mercury, which were further diluted 10-fold to circumvent lethality. Chlorpyrifos-methyl and TCDD were used at 1 µM and 100 nM, respectively, for the same reason. After 24 hours, the exposed worms were transferred to 1.5 ml tubes, washed five times with M9, and utilized for subsequent experiments and analysis through the COPAS Biosort (Union Biometrica, Holliston, MA). Time-of-flight (Tof) and GFP peak height were used as reading parameters in the COPAS Biosort. Three independent biological repeats, encompassing a total of more than 5,000 worms for each chemical exposure, were run through the COPAS Biosort. Fold-increase GFP$^+$ signal over DMSO was calculated for each biological repeat and then an average of the fold increase was calculated (Fig 1B).

Scoring embryonic lethality, larval lethality and sterility

Age-matched worms were exposed to either vehicle alone (DMSO) or each chemical in liquid for 24 hours as described above. After 24 hours, the exposed worms were washed five times with M9, and transferred to regular NGM plates to score their embryonic lethality, larval lethality and sterility. Worms were moved every 24 hours to new NGM plates (this was done for three consecutive days). The total number of fertilized eggs laid, hatched, and the number of progeny that reached adulthood were scored.

Germ cell apoptosis

Germ cell corpses were scored as in [39], utilizing a Leica DM5000B fluorescence microscope. The germlines of more than 30 worms from at least two independent biological repeats were scored for each chemical exposure. Statistical comparisons between groups were performed using the two-tailed Mann-Whitney test, 95% C.I.

Immunofluorescence microscopy

Whole mount preparation of dissected gonads and immunostainings were performed as in [67]. Primary antibodies were used at the following dilutions: goat α-SYP-1(1:3,000; [100]), rabbit α-pCHK-1(1:100; Santa Cruz), guinea pig α-pSUN-1 Ser8-pi (1:700; [65]), and rabbit α-RAD-51 (1:10,000; Novus Biological (SDI)). The following secondary antibodies from Jackson ImmunoResearch Laboratories (West Grove, PA) were used at a 1:200 dilution: α-rabbit Cy3,

and at a 1:500 dilution: α-goat Alexa 647, α-rabbit Alexa 488, and α-guinea pig Alexa 488. Vectashield from Vector Laboratories (Burlingame, CA) was used as a mounting media and anti-fading agent.

Immunofluorescence images were collected at 0.2 μm intervals with an IX-70 microscope (Olympus, Waltham, MA) and a cooled CCD camera (CH350; Roper Scientific) controlled by the Delta Vision system (Applied Precision, Pittsburgh, PA). Images were subjected to deconvolution by using the SoftWoRx 3.3.6 software (Applied Precision).

Time course analysis for RAD-51 foci

Quantitative analysis of RAD-51 foci for all seven zones composing the germline was performed as in [67]. The average number of nuclei scored per zone (n) from 3 to 6 gonads for each chemical-treated group was as follows, ± standard deviation: For the *col-121* line: zone 1 (n = 80.3±4.3), zone 2 (n = 93.5±7.4), zone 3 (n = 97.0±9.3), zone 4 (n = 86.3±6.6), zone 5 (n = 59.3±8.5), zone 6 (n = 56.5±1.7), zone 7 (n = 57.8±10.7). For the *rad-54;col-121* line: zone 1 (n = 56.5±5.8), zone 2 (n = 67.0±6.2), zone 3 (n = 59.8±5.2), zone 4 (n = 46.0±6.6), zone 5 (n = 39.8±7.8), zone 6 (n = 31.5±5.4), zone 7 (n = 26.3±2.5). Statistical comparisons were performed using the two-tailed Mann-Whitney test, 95% C.I.

RNA interference

Feeding RNAi experiments were performed at 20˚C in *col-121* mutants as described in [101] with the following modifications: three L4-stage animals were placed on each RNAi plate and F3 generation L4-stage worms were used for chemical exposures at 25˚C. HT115 bacteria expressing empty pL4440 vector was used as the control RNAi.

Strong RNAi knockdown of *spo-11* results in oocytes with 12 DAPI-stained bodies due to the lack of meiotic DSBs and subsequent crossovers leading to 6 unattached pairs of homologs. We verified that 100% (n>22) of the oocytes for each chemical exposure exhibited 12 DAPI-stained bodies. The effectiveness of RNAi was also confirmed by RT-PCR from at least four individual worms subjected to RNAi. Expression of *gpd-1* (GAPDH) transcript was used as a control.

Quantitative RT-PCR analysis

Three samples of 20 (15˚C) to 30 animals (25˚C) each were collected in 100 μl of Trizol (Invitrogen) and RNA was extracted according to the manufacturer's instructions. The extracted RNA was subjected to reverse transcription using iScript (Biorad) and quantitative real time PCR was performed using SsoFast EvaGreen supermix (Biorad) according to the manufacturer's instructions. Each sample was run in triplicate. Cq numbers were normalized to *gpd-1*, then the normalized values from DBP, permethrin, and TCMTB treated samples were statistically compared with the normalized values from vehicle (DMSO) treated samples. Bars in graphs show mean values normalized to DMSO ± SEM. Statistical comparisons were performed using the unpaired two tailed *t*-test, 95% C.I.

Live imaging

Strain CV639 (H2B::mCherry; γ-tubulin::GFP;*col-121(nx3)*) was used for live imaging and worms were immobilized with 0.01% levamisole on 3% agarose pads. Images were captured with a 60X objective every 10 seconds on an IX-70 microscope (Olympus, Waltham, MA) and a cooled CCD camera (CH350; Roper Scientific) controlled by the DeltaVision system (Applied Precision, Pittsburgh, PA).

Preparation of worm lysates for mass spectrometric analysis

After exposure to each chemical as described above, worms were washed 10 times in M9 buffer and frozen with minimal M9 in liquid nitrogen. The worm pellet was resuspended in lysis buffer [0.5 M sucrose, 25 mM HEPES (pH7.6), 5 mM EDTA, 0.5% CHAPS, 0.5% DOC (Deoxychloric acid)]. Samples were then sonicated at 4˚C for 10 cycles (1 minute on and 1 minute off per cycle) with a Bioruptor Plus 300 (Diagenode, Belgium).

Mass spectrometric chemical analysis

DBP was extracted from worms/lysates using hexane and analyzed using gas chromatography-mass spectrometry (GC-MS). A Thermo trace 1310 GC and a HP-5MS capillary column (30 m×0.25 mm×0.25 μm) interfaced with ISQ single quadrupole mass spectrometer (Waltham, MA, USA) was used for the analysis. Procedural blanks and matrix spikes were included for quality control purposes along with the analysis of control/vehicle and treated *C. elegans*. The trace level DBP found in the procedural blank was subtracted from sample values to report the final concentration. The matrix spike recovery was 91.6%.

mBP (the metabolite of DBP) in worms was analyzed using a method described for urine earlier, with some modifications [102]. Briefly, the worm lysates were enzymatically (β-glucuronidase) deconjugated followed by extraction using a solid-phase extraction (SPE) method with a solvent mixture of acetonitrile and ethyl acetate. An API 4500 electrospray QTRAP mass spectrometer (ESI-MS/MS; Applied Biosystems, AB Sciex, Framingham, MA, USA) operated in the negative mode of ionization interfaced with an Agilent 1260 HPLC (Agilent Technologies Inc., Santa Clara, CA) was used for the analysis of mBP. Quantification of mBP was achieved by an isotopic dilution method.

Permethrin was extracted from worm lysates using a similar protocol to that applied for DBP analysis. A 1:2 ratio of hexane and dichloromethane solvent mixture was used for the extraction and analysis was performed using an Agilent single quadrupole GC-MS under electron ionization mode. The matrix spike recoveries for both *cis-* and *trans*-permethrin were 112% and 101%, respectively.

For TCMTB analysis, worm lysate was spiked with 40 ng of D4-Benzothiazole (internal standard) and maintained at room temperature for equilibration (15 min). Methanol and acetone (1:1 ratio) solvent mixture was used for the extraction of target chemicals. The extracts were centrifuged and filtered through 0.2 μM nylon membrane filters and transferred into HPLC amber vials. A Shimadzu Prominence Modular HPLC system (LC-20 AD UFLC; Shimadzu Corporation, Kyoto, Japan) equipped with an Agilent Zorbax SB-Aq column (2.1 mm X 150 mm, 3.5 mm; Santa Clara, CA, USA) serially connected with an AB SCIEX 3200 triple quadrupole mass spectrometer was used for the identification and quantification of TCMTB and its metabolites (Benzothiazole (BTH), 2-methylthio benzothiazole (2-MeS BTH) and 2-hydroxy benzothiazole (2-OH BTH)) under the positive electrospray ionization mode. Although we screened for three major possible metabolites of TCMTB, we could detect only 2-MeS BTH in the treated worms. The gradient mobile phase (A: acetonitrile and B: water that contains 0.1% formic acid) was eluted at a flow rate of 300 μL/min for the effective separation of target chemicals.

Supporting information

S1 Fig. Calibration and validation of the automated fluorescence reading platform. (A) Mean number of germ cell corpses detected for DMSO (0.1%) and DBP (100 μM) exposed worms grown in the presence of either live or heat inactivated (dead) OP50 *E. coli*. There were no differences detected within DMSO or DBP groups (NS), demonstrating that the effects

were not due to the live bacteria (i.e. their response to the chemical stressor) in the media. Analysis was done for two independent biological repeats. More than 30 gonads were scored for each chemical. Error bars represent SEM. ***P<0.0001 by the two-tailed Mann-Whitney test, 95% C.I. **(B)** L2, L3, L4 and adult populations were sorted through the COPAS Biosort and used to draw a gate capturing only the adult population. The population in this gate was measured for GFP fluorescence intensity. ToF, time-of-flight. **(C)** Two genetic mutants, *Pxol-1::gfp* and *Pxol-1::gfp;him-8*, were used to define the threshold for GFP+ embryos, GFP- embryos and debris. Reading parameters used were ToF for the x-axis and GFP peak height for the y-axis. **(D)** The induction of X chromosome nondisjunction can be visualized by fluorescence microscopy. GFP+ embryos are visible within the chemical treated worm's uterus (arrows). Two chemicals that elicit increased chromosome nondisjunction, nocodazole, a microtubule disruptor, and triflumizole, a pesticide [15], were used as positive controls. Asterisks indicate gut autofluorescence.
(TIF)

S2 Fig. Chemical exposures do not affect meiotic progression. (A-D) Low magnification images of whole mounted gonads immunostained for SYP-1 (red), a central region component of the synaptonemal complex (SC), and phosphorylated SUN-1 (SUN-1 S8pi; green), a marker for progression of early prophase I events. All three chemical exposures exhibit normal timing of SC assembly and disassembly and normal duration of SUN-1 S8 signal compared to vehicle. Dissected gonads are oriented from left to right as indicated by the white arrows. Blue vertical bar indicates entrance into meiosis. Gonads are outlined to facilitate visualization. Scale bars, 10 μm. **(E)** High magnification images of mid pachytene nuclei from whole-mounted gonads immunostained for SYP-1 (red) and co-stained with DAPI (blue). Continuous full tracks of SYP-1 were observed between homologs in mid pachytene. Scale bar, 5 μm.
(TIF)

S3 Fig. Chemical exposures induce increased germ cell apoptosis in a dose-dependent manner. Chemical exposures caused a significant increase in the number of germ cell corpses observed at late pachytene compared to vehicle alone starting at 100 μM for DBP and permethrin and at 10 μM for TCMTB. Germ cell corpses from more than 30 gonads were scored for each chemical exposure. Error bars represent SEM. **P<0.01, ***P<0.0001 by the two-tailed Mann-Whitney test, 95% C.I.
(TIF)

S4 Fig. Elevated meiotic DSB levels observed following chemical exposures are SPO-11-dependent. (A, B) Representative images of pachytene nuclei (z5) immunostained for RAD-51 (red), co-stained with DAPI (blue) and high magnification images of oocytes at diakinesis positioned right before the spermatheca (-1 oocyte) in *col-121* control (empty vector) RNAi (A) or *col-121 spo-11(RNAi)* (B). Six bivalents are observed in 100% (n = DMSO: 11, DBP: 10, permethrin: 25, and TCMTB: 18) of the oocytes scored in control RNAi. In contrast, 12 univalents are observed in 100% (n = DMSO: 28, DBP: 29, permethrin: 25, and TCMTB: 22) of the -1 oocytes upon SPO-11 depletion indicating that RNAi depletion worked effectively. While elevated levels of RAD-51 foci are observed in pachytene nuclei for all indicated chemical exposures compared with control, scarcely any RAD-51 foci are observed in pachytene nuclei for either the chemical exposures or vehicle alone when SPO-11 is depleted. Scale bar, 5 μm. **(C)** Histograms show the mean number of RAD-51 foci scored per nucleus for each zone from *col-121* control(RNAi) (C) and *col-121 spo-11(RNAi)* worms (D). Three gonads from two independent biological repeats were scored for each indicated exposure. Error bars represent SEM. *P<0.05, **P<0.01, ***P<0.001 by the two-tailed Mann-Whitney test, 95% C.

I. **(D)** RT-PCR of *col-121 spo-11(RNAi)* compared to *col-121 control(RNAi)* (empty vector). Each lane corresponds to a single worm lysate and indicates the effective depletion of *spo-11* by RNAi (shown are the single worm lysates from vehicle alone). *gpd-1* expression was used as a loading control.
(TIF)

S1 Table. Readouts from high-throughput screening of the environmental chemicals with the COPAS Biosort. Categories indicate the class or use of the chemicals tested (pesticide, phthalate, crude oil processing and hydraulic fracturing; exceptions are TCDD and BPA listed as dioxin and plasticizer, respectively). Concentrations assessed for each chemical in the high-throughput screen are indicated (all chemicals were diluted in DMSO). Chemicals are ranked based on the fold increase in GFP$^+$ embryos detected compared with DMSO-treated (vehicle alone) worms. A minimum of 5,000 worms were screened for each chemical.
(TIF)

S2 Table. Raw data set. Raw data for plate phenotyping, apoptotic nuclei count, RAD-51 foci count, and qRT-PCR analysis.
(XLSX)

Author Contributions

Conceptualization: Monica P. Colaiácovo.

Formal analysis: Nara Shin, Rajendiran Karthikraj.

Funding acquisition: Monica P. Colaiácovo.

Investigation: Nara Shin.

Methodology: Nara Shin, Luciann Cuenca, Rajendiran Karthikraj, Kurunthachalam Kannan.

Project administration: Monica P. Colaiácovo.

Resources: Luciann Cuenca.

Supervision: Monica P. Colaiácovo.

Writing – original draft: Nara Shin, Monica P. Colaiácovo.

Writing – review & editing: Nara Shin, Rajendiran Karthikraj, Kurunthachalam Kannan, Monica P. Colaiácovo.

References

1. Siracusa JS, Yin L, Measel E, Liang S, Yu X. Effects of bisphenol A and its analogs on reproductive health: A mini review. Reprod Toxicol. 2018; 79: 96–123. https://doi.org/10.1016/j.reprotox.2018.06.005 PMID: 29925041

2. Noorimotlagh Z, Haghighi NJ, Ahmadimoghadam M, Rahim F. An updated systematic review on the possible effect of nonylphenol on male fertility. EnvironSci -Pollut Res. 2017; 24: 3298–3314. https://doi.org/10.1007/s11356-016-7960-y PMID: 27826822

3. Tomza-Marciniak A, Stępkowska P, Kuba J, Pilarczyk B. Effect of bisphenol A on reproductive processes: A review of *in vitro*, *in vivo* and epidemiological studies: Effect of BPA on reproductive processes. J Appl Toxicol. 2018; 38: 51–80. https://doi.org/10.1002/jat.3480 PMID: 28608465

4. Del-Mazo J, Brieño-Enríquez MA, García-López J, López-Fernández LA, De-Felici M. Endocrine disruptors, gene deregulation and male germ cell tumors. IntJ Dev Biol. 2013; 57: 225–239. https://doi.org/10.1387/ijdb.130042jd PMID: 23784834

5. Brieño-Enríquez MA, Larriba E, del Mazo J. Endocrine disrupters, microRNAs, and primordial germ cells: a dangerous cocktail. Fertil Steril. 2016; 106: 871–879. https://doi.org/10.1016/j.fertnstert.2016.07.1100 PMID: 27521771

6. Hunt PA, Hassold TJ. Human female meiosis: what makes a good egg go bad? Trends Genet. 2008; 24: 86–93. https://doi.org/10.1016/j.tig.2007.11.010 PMID: 18192063

7. Nagaoka SI, Hassold TJ, Hunt PA. Human aneuploidy: mechanisms and new insights into an age-old problem. Nat Rev Genet. 2012; 13: 493–504. https://doi.org/10.1038/nrg3245 PMID: 22705668

8. Leung MCK, Williams PL, Benedetto A, Au C, Helmcke KJ, Aschner M, et al. *Caenorhabditis elegans*: An emerging model in biomedical and environmental toxicology. Toxicol Sci. 2008; 106: 5–28. https://doi.org/10.1093/toxsci/kfn121 PMID: 18566021

9. Lui DY, Colaiácovo MP. Meiotic development in *Caenorhabditis elegans*. In: Schedl T, editor. Germ Cell Development in C elegans. New York, NY: Springer New York; 2013. pp. 133–170. https://doi.org/10.1007/978-1-4614-4015-4_6

10. Ferreira DW, Allard P. Models of germ cell development and their application for toxicity studies. Environ Mol Mutagen. 2015; 56: 637–649. https://doi.org/10.1002/em.21946 PMID: 25821157

11. Lucanic M, Garrett T, Gill MS, Lithgow GJ. A simple method for high throughput chemical screening in *Caenorhabditis Elegans*. J Vis Exp. 2018; https://doi.org/10.3791/56892 PMID: 29630057

12. Colaiácovo MP. The many facets of SC function during *C. elegans* meiosis. Chromosoma. 2006; 115: 195–211. https://doi.org/10.1007/s00412-006-0061-9 PMID: 16555015

13. O'Reilly LP, Luke CJ, Perlmutter DH, Silverman GA, Pak SC. *C. elegans* in high-throughput drug discovery. Adv Drug Deliv Rev. 2014; 69–70: 247–253. https://doi.org/10.1016/j.addr.2013.12.001 PMID: 24333896

14. Kaletta T, Hengartner MO. Finding function in novel targets: *C. elegans* as a model organism. Nat Rev Drug Discov. 2006; 5: 387–399. https://doi.org/10.1038/nrd2031 PMID: 16672925

15. Allard P, Kleinstreuer NC, Knudsen TB, Colaiácovo MP. A *C. elegans* screening platform for the rapid assessment of chemical disruption of germline function. Environ Health Perspect. 2013; 121: 717–724. https://doi.org/10.1289/ehp.1206301 PMID: 23603051

16. Allard P, Colaiácovo MP. Bisphenol A impairs the double-strand break repair machinery in the germline and causes chromosome abnormalities. Proc Natl Acad Sci U S A. 2010; 107: 20405–20410. https://doi.org/10.1073/pnas.1010386107 PMID: 21059909

17. Hunt PA, Koehler KE, Susiarjo M, Hodges CA, Ilagan A, Voigt RC, et al. Bisphenol A exposure causes meiotic aneuploidy in the female mouse. Curr Biol. 2003; 13: 546–553. https://doi.org/10.1016/S0960-9822(03)00189-1 PMID: 12676084

18. Susiarjo M, Hassold TJ, Freeman E, Hunt PA. Bisphenol A exposure *in utero* disrupts early oogenesis in the mouse. PLoS Genet. 2007; 3: e5. https://doi.org/10.1371/journal.pgen.0030005 PMID: 17222059

19. Brieño-Enríquez MA, Robles P, Camats-Tarruella N, García-Cruz R, Roig I, Cabero L, et al. Human meiotic progression and recombination are affected by Bisphenol A exposure during *in vitro* human oocyte development. Hum Reprod. 2011; 26: 2807–2818. https://doi.org/10.1093/humrep/der249 PMID: 21795248

20. Lawson C, Gieske M, Murdoch B, Ye P, Li Y, Hassold T, et al. Gene expression in the fetal mouse ovary is altered by exposure to low doses of Bisphenol A. Biol of Reprod. 2011; 84: 79–86. https://doi.org/10.1095/biolreprod.110.084814 PMID: 20739668

21. Hines CJ, Hopf NBN, Deddens JA, Silva MJ, Calafat AM. Estimated daily intake of phthalates in occupationally exposed groups. J Expo Sci Environ Epidemiol. 2011; 21: 133–141. https://doi.org/10.1038/jes.2009.62 PMID: 20010977

22. Kavlock R, Boekelheide K, Chapin R, Cunningham M, Faustman E, Foster P, et al. NTP center for the evaluation of risks to human reproduction: phthalates expert panel report on the reproductive and developmental toxicity of di-n-butyl phthalate. Reprod Toxicol. 2002; 39.

23. Guo Y, Kannan K. A survey of phthalates and parabens in personal care products from the United States and its implications for human exposure. Environ Sci Technol. 2013; 47: 14442–14449. https://doi.org/10.1021/es4042034 PMID: 24261694

24. Gao C-J, Liu L-Y, Ma W-L, Ren N-Q, Guo Y, Zhu N-Z, et al. Phthalate metabolites in urine of Chinese young adults: Concentration, profile, exposure and cumulative risk assessment. Sci Total Environ. 2016; 543: 19–27. https://doi.org/10.1016/j.scitotenv.2015.11.005 PMID: 26575634

25. Okayama Y, Wakui S, Wempe MF, Sugiyama M, Motohashi M, Mutou T, et al. *In Utero* exposure to Di (*n* -butyl)phthalate induces morphological and biochemical changes in rats postpuberty. Toxicol Pathol. 2017; 45: 526–535. https://doi.org/10.1177/0192623317709091 PMID: 28641505

26. Wang H, Wang J, Zhang J, Jin S, Li H. Role of PI3K/AKT/mTOR signaling pathway in DBP-induced apoptosis of testicular sertoli cells *in vitro*. Environ Toxicol Pharmacol. 2017; 53: 145–150. https://doi.org/10.1016/j.etap.2017.05.013 PMID: 28578144

27. Sen N, Liu X, Craig ZR. Short term exposure to di-n-butyl phthalate (DBP) disrupts ovarian function in young CD-1 mice. Reprod Toxicol. 2015; 53: 15–22. https://doi.org/10.1016/j.reprotox.2015.02.012 PMID: 25765776

28. Rasmussen LM, Sen N, Vera JC, Liu X, Craig ZR. Effects of *in vitro* exposure to dibutyl phthalate, mono-butyl phthalate, and acetyl tributyl citrate on ovarian antral follicle growth and viability. Biol Reprod. 2017; 96: 1105–1117. https://doi.org/10.1095/biolreprod.116.144691 PMID: 28486587

29. Swan SH, Main KM, Liu F, Stewart SL, Kruse RL, Calafat AM, et al. Decrease in anogenital distance among male infants with prenatal phthalate exposure. Environ Health Perspect. 2005; 113: 1056–1061. https://doi.org/10.1289/ehp.8100 PMID: 16079079

30. Keenan JJ, Ross JH, Sell V, Vega HM, Krieger RI. Deposition and spatial distribution of insecticides following fogger, perimeter sprays, spot sprays, and crack-and-crevice applications for treatment and control of indoor pests. Regul Toxicol Pharmacol. 2010; 58: 189–195. https://doi.org/10.1016/j.yrtph.2010.05.003 PMID: 20472011

31. Barr DB, Olsson AO, Wong L-Y, Udunka S, Baker SE, Whitehead RD, et al. Urinary concentrations of metabolites of pyrethroid insecticides in the general U.S. population: National health and nutrition examination survey 1999–2002. Environ Health Perspect. 2010; 118: 742–748. https://doi.org/10.1289/ehp.0901275 PMID: 20129874

32. Egeghy PP, Cohen Hubal EA, Tulve NS, Melnyk LJ, Morgan MK, Fortmann RC, et al. Review of pesticide urinary biomarker measurements from selected US EPA children's observational exposure studies. Int J Environ Res Public Health. 2011; 8: 1727–1754. https://doi.org/10.3390/ijerph8051727 PMID: 21655147

33. Ding Y, Landrum PF, You J, Lydy MJ. Assessing bioavailability and toxicity of permethrin and DDT in sediment using matrix solid phase microextraction. Ecotoxicology. 2013; 22: 109–117. https://doi.org/10.1007/s10646-012-1007-z PMID: 23086182

34. Morgan MK. Children's exposures to pyrethroid insecticides at home: A review of data collected in published exposure measurement studies conducted in the United States. Int J Environ Res Public Health. 2012; 9: 2964–2985. https://doi.org/10.3390/ijerph9082964 PMID: 23066409

35. Neta G, Goldman LR, Barr D, Sjödin A, Apelberg BJ, Witter FR, et al. Distribution and determinants of pesticide mixtures in cord serum using principal component analysis. Environ Sci Technol. 2010; 44: 5641–5648. https://doi.org/10.1021/es1009778 PMID: 20550184

36. Navarrete-Meneses MP, Salas-Labadía C, Sanabrais-Jiménez M, Santana-Hernández J, Serrano-Cuevas A, Juárez-Velázquez R, et al. "Exposure to the insecticides permethrin and malathion induces leukemia and lymphoma-associated gene aberrations *in vitro*." Toxicol In Vitro. 2017; 44: 17–26. https://doi.org/10.1016/j.tiv.2017.06.013 PMID: 28624474

37. Liao C, Kim U-J, Kannan K. A review of environmental occurrence, fate, exposure, and toxicity of benzothiazoles. Environ Sci Technol. 2018; 52: 5007–5026. https://doi.org/10.1021/acs.est.7b05493 PMID: 29578695

38. Hodgkin J, Horvitz HR, Brenner S. Nondisjunction mutants of the nematode *Caenorhabditis elegans*. Genetics. 1979; 91: 67–94 PMID: 17248881

39. Kelly KO, Dernburg AF, Stanfield GM, Villeneuve AM. *Caenorhabditis elegans msh-5* is required for both normal and radiation-induced meiotic crossing over but not for completion of meiosis. Genetics. 2000; 156 617–630. PMID: 11014811

40. Miller LM, Plenefisch JD, Casson LR, Meyer BJ. *xol-1*: A gene that controls the male modes of both sex determination and X chromosome dosage compensation in *C. elegans*. Cell. 1988; 55: 167–183. PMID: 3167975

41. Watanabe M, Mitani N, Ishii N, Miki K. A mutation in a cuticle collagen causes hypersensitivity to the endocrine disrupting chemical, bisphenol A, in *Caenorhabditis elegans*. Mutat Res. 2005; 570: 71–80. https://doi.org/10.1016/j.mrfmmm.2004.10.005 PMID: 15680404

42. Boyd WA, McBride SJ, Rice JR, Snyder DW, Freedman JH. A high-throughput method for assessing chemical toxicity using a *Caenorhabditis elegans* reproduction assay. Toxicol Appl Pharmacol. 2010; 245: 153–159. https://doi.org/10.1016/j.taap.2010.02.014 PMID: 20206647

43. Boyd WA, Smith MV, Kissling GE, Freedman JH. Medium- and high-throughput screening of neurotoxicants using *C. elegans*. Neurotoxicol Teratol. 2010; 32: 68–73. https://doi.org/10.1016/j.ntt.2008.12.004 PMID: 19166924

44. Rice KM, Walker EM, Wu M, Gillette C, Blough ER. Environmental mercury and its toxic effects. J Prev Med Public Health. 2014; 47: 74–83. https://doi.org/10.3961/jpmph.2014.47.2.74 PMID: 24744824

45. Reutman SR, LeMasters GK, Knecht EA, Shukla R, Lockey JE, Burroughs GE, et al. Evidence of reproductive endocrine effects in women with occupational fuel and solvent exposures. Environ Health Perspect. 2002; 110: 805–811. https://doi.org/10.1289/ehp.02110805 PMID: 12153763

46. Niaz K, Bahadar H, Maqbool F, Abdollahi M. A review of environmental and occupational exposure to xylene and its health concerns. EXCLI J. 2015; https://doi.org/10.17179/excli2015-623 PMID: 26862322

47. Heres-Pulido ME, Lombera-Hernández S, Dueñas-García I, Perales-Canales I, Castañeda-Partida L, Rocha-Ortiz C, et al. Genotoxicity of triasulfuron in the wing spot test of *Drosophila melanogaster* is modulated by winter wheat seedlings. Mutat Res. 2008; 653: 70–75. https://doi.org/10.1016/j.mrgentox.2008.03.005 PMID: 18468945

48. Dimitrov BD, Gadeva PG, Benova DK, Bineva MV. Comparative genotoxicity of the herbicides Roundup, Stomp and Reglone in plant and mammalian test systems. Mutagenesis. 2006; 21: 375–382. https://doi.org/10.1093/mutage/gel044 PMID: 16998229

49. Delescluse C, Ledirac N, Li R, Piechocki MP, Hines RN, Gidrol X, et al. Induction of cytochrome P450 1A1 gene expression, oxidative stress, and genotoxicity by carbaryl and thiabendazole in transfected human HepG2 and lymphoblastoid cells. Biochem Pharmacol. 2001; 61: 399–407. PMID: 11226373

50. Mailhes JB, Young D, Aardema MJ, London SN. Thiabendazole-induced cytogenetic abnormalities in mouse oocytes. Environ Mol Mutagen. 1997; 29: 367–371. https://doi.org/10.1002/(SICI)1098-2280(1997)29:4<367::AID-EM4>3.0.CO;2–7 PMID: 9212787

51. Schmid TE, Wang Xu, Adler I.-D. Detection of aneuploidy by multicolor FISH in mouse sperm after *in vivo* treatment with acrylamide, colchicine, diazepam or thiabendazole. Mutagenesis. 1999; 14: 173–179. https://doi.org/10.1093/mutage/14.2.173 PMID: 10229918

52. Hayashi S, Taketa Y, Inoue K, Takahashi M, Matsuo S, Irie K, et al. Effects of pyperonyl butoxide on the female reproductive tract in rats. J Toxicol Sci. 2013; 38: 891–902. https://doi.org/10.2131/jts.38.891 PMID: 24213009

53. Lyche JL, Gutleb AC, Bergman Å, Eriksen GS, Murk AJ, Ropstad E, et al. Reproductive and Developmental Toxicity of Phthalates. J Toxicol Environ Health. 2009; 12: 225–249. https://doi.org/10.1080/10937400903094091 PMID: 20183522

54. Bloom MS, Whitcomb BW, Chen Z, Ye A, Kannan K, Buck Louis GM. Associations between urinary phthalate concentrations and semen quality parameters in a general population. Hum Reprod. 2015; 30: 2645–2657. https://doi.org/10.1093/humrep/dev219 PMID: 26350610

55. Matsumoto M, Hirata-Koizumi M, Ema M. Potential adverse effects of phthalic acid esters on human health: A review of recent studies on reproduction. Regul Toxicol Pharmacol. 2008; 50: 37–49. https://doi.org/10.1016/j.yrtph.2007.09.004 PMID: 17983696

56. Smarr MM, Kannan K, Sun L, Honda M, Wang W, Karthikraj R, et al. Preconception seminal plasma concentrations of endocrine disrupting chemicals in relation to semen quality parameters among male partners planning for pregnancy. Environ Res. 2018; 167: 78–86. https://doi.org/10.1016/j.envres.2018.07.004 PMID: 30014899

57. Duty SM, Singh NP, Silva MJ, Barr DB, Brock JW, Ryan L, et al. The relationship between environmental exposures to phthalates and DNA damage in human sperm using the neutral comet assay. Environ Health Perspect. 2003; 111: 1164–1169. https://doi.org/10.1289/ehp.5756 PMID: 12842768

58. Hauser R. Urinary phthalate metabolites and semen quality: a review of a potential biomarker of susceptibility. Int J Androl. 2008; 31: 112–117. https://doi.org/10.1111/j.1365-2605.2007.00844.x PMID: 18067563

59. Hauser R, Meeker JD, Singh NP, Silva MJ, Ryan L, Duty S, et al. DNA damage in human sperm is related to urinary levels of phthalate monoester and oxidative metabolites. Hum Reprod. 2007; 22: 688–695. https://doi.org/10.1093/humrep/del428 PMID: 17090632

60. Rozati R, Reddy P., Reddanna P, Mujtaba R. Role of environmental estrogens in the deterioration of male factor fertility. Fertil Steril. 2002; 78: 1187–1194. https://doi.org/10.1016/S0015-0282(02)04389-3 PMID: 12477510

61. Zhang T, Li L, Qin X-S, Zhou Y, Zhang X-F, Wang L-Q, et al. Di-(2-ethylhexyl) phthalate and bisphenol A exposure impairs mouse primordial follicle assembly *in vitro*: DEHP and BPA impairs mouse primordial follicle assembly. Environ Mol Mutagen. 2014; 55: 343–353. https://doi.org/10.1002/em.21847 PMID: 24458533

62. Pocar P, Fiandanese N, Berrini A, Secchi C, Borromeo V. Maternal exposure to di(2-ethylhexyl)phthalate (DEHP) promotes the transgenerational inheritance of adult-onset reproductive dysfunctions through the female germline in mice. Toxicol Appl Pharmacol. 2017; 322: 113–121. https://doi.org/10.1016/j.taap.2017.03.008 PMID: 28286118

63. Balise VD, Meng C-X, Cornelius-Green JN, Kassotis CD, Kennedy R, Nagel SC. Systematic review of the association between oil and natural gas extraction processes and human reproduction. Fertil Steril. 2016; 106: 795–819. https://doi.org/10.1016/j.fertnstert.2016.07.1099 PMID: 27568524

64. Gartner A, Milstein S, Ahmed S, Hodgkin J, Hengartner MO. A conserved checkpoint pathway mediates DNA damage–induced apoptosis and cell cycle arrest in *C. elegans*. Mol Cell. 2000; 5: 435–443. https://doi.org/10.1016/S1097-2765(00)80438-4 PMID: 10882129

65. Woglar A, Daryabeigi A, Adamo A, Habacher C, Machacek T, La Volpe A, et al. Matefin/SUN-1 phosphorylation is part of a surveillance mechanism to coordinate chromosome synapsis and recombination with meiotic progression and chromosome movement. PLoS Genet. 2013; 9: e1003335. https://doi.org/10.1371/journal.pgen.1003335 PMID: 23505384

66. MacQueen AJ. Synapsis-dependent and -independent mechanisms stabilize homolog pairing during meiotic prophase in *C. elegans*. Genes Dev. 2002; 16: 2428–2442. https://doi.org/10.1101/gad.1011602 PMID: 12231631

67. Colaiácovo MP, MacQueen AJ, Martinez-Perez E, McDonald K, Adamo A, La Volpe A, et al. Synaptonemal complex assembly in *C. elegans* is dispensable for loading strand-exchange proteins but critical for proper completion of recombination. Dev Cell. 2003; 5: 463–474. https://doi.org/10.1016/S1534-5807(03)00232-6 PMID: 12967565

68. Gumienny TL. Lambie E, Hartwieg E, Horvitz HR, Hengartner MO. Genetic control of programmed cell death in the *Caenorhabditis elegans* hermaphrodite germline. Development. 1999; 126: 1011–1022 PMID: 9927601

69. Schumacher B, Hofmann K, Boulton S, Gartner A. The *C. elegans* homolog of the p53 tumor suppressor is required for DNA damage-induced apoptosis. Curr Biol. 2001; 11: 1722–1727. https://doi.org/10.1016/S0960-9822(01)00534-6 PMID: 11696333

70. Moser SC, von Elsner S, Büssing I, Alpi A, Schnabel R, Gartner A. Functional dissection of *Caenorhabditis elegans* CLK-2/TEL2 cell cycle defects during embryogenesis and germline development. PLoS Genet. 2009; 5: e1000451. https://doi.org/10.1371/journal.pgen.1000451 PMID: 19360121

71. Sung P. Catalysis of ATP-dependent homologous DNA pairing and strand exchange by yeast RAD51 protein. Science. 1994; 265: 1241–1243 PMID: 8066464

72. Mets DG, Meyer BJ. Condensins regulate meiotic DNA break distribution, thus crossover frequency, by controlling chromosome structure. Cell. 2009; 139: 73–86. https://doi.org/10.1016/j.cell.2009.07.035 PMID: 19781752

73. Austin J, Kimble J. *glp-1* is required in the germ line for regulation of the decision between mitosis and meiosis in *C. elegans*. Cell. 1987; 51: 589–599 PMID: 3677168

74. Jansson M, Durant ST, Cho E-C, Sheahan S, Edelmann M, Kessler B, et al. Arginine methylation regulates the p53 response. Nat Cell Biol. 2008; 10: 1431–1439. https://doi.org/10.1038/ncb1802 PMID: 19011621

75. Yang M, Sun J, Sun X, Shen Q, Gao Z, Yang C. *Caenorhabditis elegans* protein arginine methyltransferase PRMT-5 negatively regulates DNA damage-induced apoptosis. PLoS Genet. 2009; 5: e1000514. https://doi.org/10.1371/journal.pgen.1000514 PMID: 19521535

76. Duronio RJ, O'Farrell PH, Sluder G, Su TT. Sophisticated lessons from simple organisms: appreciating the value of curiosity-driven research. Dis Model Mech. 2017; 10: 1381–1389. https://doi.org/10.1242/dmm.031203 PMID: 29259023

77. Lees H, Walters H, Cox LS. Animal and human models to understand ageing. Maturitas. 2016; 93: 18–27. https://doi.org/10.1016/j.maturitas.2016.06.008 PMID: 27372369

78. van der Bliek AM, Sedensky MM, Morgan PG. Cell biology of the mitochondrion. Genetics. 2017; 207: 843–871. https://doi.org/10.1534/genetics.117.300262 PMID: 29097398

79. Li J, Le W. Modeling neurodegenerative diseases in *Caenorhabditis elegans*. Exp Neurol. 2013; 250: 94–103. https://doi.org/10.1016/j.expneurol.2013.09.024 PMID: 24095843

80. Stuelten CH, Parent CA, Montell DJ. Cell motility in cancer invasion and metastasis: insights from simple model organisms. Nat Rev Cancer. 2018; 18: 296–312. https://doi.org/10.1038/nrc.2018.15 PMID: 29546880

81. Hunt PR. The *C. elegans* model in toxicity testing. J Appl Toxicol. 2017; 37: 50–59. https://doi.org/10.1002/jat.3357 PMID: 27443595

82. Ke W, Drangowska-Way A, Katz D, Siller K, O'Rourke EJ. The ancient genetic networks of obesity: Whole-animal automated screening for conserved fat regulators. In: Wagner B, editor. Phenotypic

Screening. New York, NY: Springer New York; 2018. pp. 129–146. https://doi.org/10.1007/978-1-4939-7847-2_10

83. Peterson ND, Pukkila-Worley R. *Caenorhabditis elegans* in high-throughput screens for anti-infective compounds. Curr Op Immunol. 2018; 54: 59–65. https://doi.org/10.1016/j.coi.2018.06.003 PMID: 29935375

84. Crow J, Borazjani A, Potter P, Ross M. Hydrolysis of pyrethroids by human and rat tissues: Examination of intestinal, liver and serum carboxylesterases. Toxicol Appl Pharmacol. 2007; 221: 1–12. https://doi.org/10.1016/j.taap.2007.03.002 PMID: 17442360

85. Scollon EJ, Starr JM, Godin SJ, DeVito MJ, Hughes MF. *In Vitro* metabolism of pyrethroid pesticides by rat and human hepatic microsomes and cytochrome P450 isoforms. Drug Metabolism and Disposition. 2009; 37: 221–228. https://doi.org/10.1124/dmd.108.022343 PMID: 18948380

86. Ratelle M, Coté J, Bouchard M. Time profiles and toxicokinetic parameters of key biomarkers of exposure to cypermethrin in orally exposed volunteers compared with previously available kinetic data following permethrin exposure: Toxicokinetics of cypermethrin and permethrin biomarkers. J Appl Toxicol. 2015; 35: 1586–1593. https://doi.org/10.1002/jat.3124 PMID: 25772368

87. Manninen A, Auriola S, Vartiainen M, Liesivuori J, Turunen T, Pasanen M. Determination of urinary 2-mercaptobenzothiazole (2-MBT), the main metabolite of 2-(thiocyanomethylthio)benzothiazole (TCMTB) in humans and rats. Arch Toxicol. 1996; 70: 579–584. https://doi.org/10.1007/s002040050315 PMID: 8831908

88. Krotz SP, Carson SA, Tomey C, Buster JE. Phthalates and bisphenol do not accumulate in human follicular fluid. J Assist Reprod Genet. 2012; 29: 773–777. https://doi.org/10.1007/s10815-012-9775-1 PMID: 22538552

89. Du Y-Y, Fang Y-L, Wang Y-X, Zeng Q, Guo N, Zhao H, et al. Follicular fluid and urinary concentrations of phthalate metabolites among infertile women and associations with *in vitro* fertilization parameters. Reprod Toxicol. 2016; 61: 142–150. https://doi.org/10.1016/j.reprotox.2016.04.005 PMID: 27067915

90. Bornehag C-G, Carlstedt F, Jönsson BA, Lindh CH, Jensen TK, Bodin A, et al. Prenatal phthalate exposures and anogenital distance in Swedish boys. Environ Health Perspect. 2015; 123: 101–107. https://doi.org/10.1289/ehp.1408163 PMID: 25353625

91. Bowitch A, Michaels KL, Yu MC, Ferkey DM. The protein arginine methyltransferase PRMT-5 Regulates SER-2 tyramine receptor-mediated behaviors in *Caenorhabditis elegans*. G3(Bethesda). 2018; 8: 2389–2398. https://doi.org/10.1534/g3.118.200360 PMID: 29760200

92. Hartsuiker E, Mizuno K, Molnar M, Kohli J, Ohta K, Carr AM. Ctp1CtIP and Rad32Mre11 nuclease activity are required for Rec12Spo11 removal, but Rec12Spo11 removal is dispensable for other MRN-dependent meiotic functions. Mol Cell Biol. 2009; 29: 1671–1681. https://doi.org/10.1128/MCB.01182-08 PMID: 19139281

93. Puizina J. Mre11 deficiency in Arabidopsis is associated with chromosomal instability in somatic cells and Spo11-dependent genome fragmentation during meiosis. Plant Cell. 2004; 16: 1968–1978. https://doi.org/10.1105/tpc.104.022749 PMID: 15258261

94. Johzuke K, Ogawa H. Interaction of Mre11 and Rad50: two proteins required for DNA repair and meiosis-specific double-strand break formation in *Saccharomyces cerevisiae*. Genetics. 1995; 139: 1521–1532 PMID: 7789757

95. Yin Y, Smolikove S. Impaired resection of meiotic double-strand breaks channels repair to Nonhomologous End Joining in *Caenorhabditis elegans*. Mol Cell Biol. 2013; 33: 2732–2747. https://doi.org/10.1128/MCB.00055-13 PMID: 23671188

96. Tsubouchi H, Ogawa H. A Novel *mre11* mutation impairs processing of double-strand breaks of DNA during both mitosis and meiosis. Mol Cell Biol. 1998; 18: 260–268. https://doi.org/10.1128/MCB.18.1.260 PMID: 9418873

97. Young JA, Hyppa RW, Smith GR. Conserved and nonconserved proteins for meiotic DNA breakage and repair in yeasts. Genetics. 2004; 167: 593–605. https://doi.org/10.1534/genetics.103.023762 PMID: 15238514

98. Brenner S. The genetics of *Caenorhabditis elegans*. Genetics. 1974; 77:71–94 PMID: 4366476

99. Stiernagle T. Maintenance of *C. elegans*. WormBook. 2006; https://doi.org/10.1895/wormbook.1.101.1 PMID: 18050451

100. Nadarajan S, Lambert TJ, Altendorfer E, Gao J, Blower MD, Waters JC, et al. Polo-like kinase-dependent phosphorylation of the synaptonemal complex protein SYP-4 regulates double-strand break formation through a negative feedback loop. eLife. 2017; 6: e23437. https://doi.org/10.7554/eLife.23437 PMID: 28346135

101. Govindan JA, Cheng H, Harris JE, Greenstein D. Gαo/i and Gαs signaling function in parallel with the MSP/Eph receptor to control meiotic diapause in *C. elegans*. Curr Biol. 2006; 16: 1257–1268. https://doi.org/10.1016/j.cub.2006.05.020 PMID: 16824915

102. Guo Y, Alomirah H, Cho H-S, Minh TB, Mohd MA, Nakata H, et al. Occurrence of phthalate metabolites in human urine from several Asian countries. Environ Sci Technol. 2011; 45: 3138–3144. https://doi.org/10.1021/es103879m PMID: 21395215

103. Goldstein P, Magnano L, Rojo J. Effects of dimethyl sulfone (DMSO2) on early gametogenesis in *Caenorhabditis elegans*: ultrastructural aberrations and loss of synaptonemal complexes from pachytene nuclei. Reprod Toxicol. 1992; 6: 149–159. https://doi.org/10.1016/0890-6238(92)90117-C PMID: 1591472